Available online at www.sciencedirect.com

ScienceDirect

Polymer 48 (2007) 6965–6991

polymer

www.elsevier.com/locate/polymer

Feature Article

Emulsion polymerization: State of the art in kinetics and mechanisms

Stuart C. Thickett [a], Robert G. Gilbert [b,*]

[a] Key Centre for Polymer Colloids, Chemistry School F11, The University of Sydney, NSW 2006, Australia
[b] CNAFS/LCAFS, Hartley Teakle Bldg S434, The University of Queensland, Brisbane, QLD 4072, Australia

Received 16 May 2007; received in revised form 30 July 2007; accepted 16 September 2007
Available online 26 September 2007

Abstract

Over decades of carefully designed kinetic experiments and the development of complementary theory, a more or less complete picture of the mechanisms that govern emulsion polymerization systems has been established. This required means of determining the rate coefficients for the individual processes as functions of controllable variables such as initiator concentration and particle size, means of interpreting the data with a minimum of model-based assumptions, and the need to perform experiments that had the potential to actually refute a given mechanistic hypothesis. Significant advances have been made within the area of understanding interfacial processes such as radical entry and exit into and out of an emulsion polymerization particle, for electrostatic, steric and electrosteric stabilizers (the latter two being poorly understood until recently). The mechanism for radical exit is chain transfer to monomer within the particle interior to form a monomeric radical which can either diffuse into the water phase or propagate to form a more hydrophobic species which cannot exit. Entry is through aqueous-phase propagation of a radical derived directly from initiator, until a critical degree of polymerization z is reached; the value of z is such that the z-meric species is sufficiently surface active so that its only fate is to enter, whereas smaller aqueous-phase radical species can either be terminated in the aqueous phase or undergo further propagation. For both entry and exit, in the presence of (electro)steric stabilizers, two additional events are significant: transfer involving a labile hydrogen atom within the stabilizing layer to form a mid-chain radical which is slow to propagate and quick to terminate, and which may also undergo β-scission to form a water-soluble species. Proper consideration of the fates of the various aqueous-phase radicals is essential for understanding the overall kinetic behaviour. Intra-particle termination is explained in terms of diffusion-controlled chain-length-dependent events. A knowledge of the events controlling entry and exit, including the recent discoveries of the additional mechanisms operating with (electro)steric stabilizers, provides an extension to the micellar and homogeneous nucleation models which enables particle number to be predicted with acceptable reliability, and also quantifies the amount of secondary nucleation occurring during seeded growth. This knowledge provides tools to understand the kinetics of emulsion polymerization, in both conventional and controlled/living polymerization systems, and to optimize reaction conditions to synthesize better polymer products.

Keywords: Emulsion polymerization; Kinetics; Mechanism

1. Introduction

Emulsion polymerization is the commonest way of forming polymer latexes; in the simplest system, the ingredients comprise water, a monomer of low water solubility (e.g. styrene), water-soluble initiator (e.g. persulfate) and surfactant (latexes can also be synthesized without added surfactant and/or initiator, but these are not common). A new phase quickly forms: a polymer colloid, comprising a discrete phase of colloidally stable latex particles, dispersed in an aqueous continuous phase. Virtually all polymerization occurs within these nanoreactors. By the end of the reaction, these are typically $\sim 10^2$ nm in size, each containing many polymer chains. Colloidal stabilizers may be electrostatic (e.g. with an ionic surfactant such as sodium dodecyl sulfate), steric (with a steric, or polymeric, stabilizer such as poly(ethylene oxide) nonylphenyl ether), or electrosteric, displaying both stabilizing mechanisms, such as a 'hairy layer' of poly(acrylic acid) grafted to long hydrophobic chains within the particles.

* Corresponding author. Tel.: +61 7 3365 4809; fax: +61 7 3365 1188.
E-mail address: b.gilbert@uq.edu.au (R.G. Gilbert).

0032-3861
doi:10.1016/j.polymer.2007.09.031

Emulsion polymerization is a widely used technique industrially to synthesize large quantities of latex for a multitude of applications such as surface coatings (paints, adhesives,…) and bulk polymer (poly(styrene-*co*-butadiene), polychlorobutadiene,…) [1], and has a number of technical advantages. The use of water as the dispersion medium is environmentally friendly (compared to using volatile organic solvents) and also allows excellent heat dissipation during the course of the polymerization. Similarly, the low viscosity of the emulsion allows access to high weight fractions of polymer not readily accessible in solution or bulk polymerization reactions. The fact that radicals are compartmentalized within particles and hence cannot terminate with a polymeric radical within another particle can, under certain circumstances, give higher polymerization rates and molecular weights than that are normally achievable in solution [2].

Despite these advantages and the relative simplicity of the process, emulsion polymerization involves many mechanistic events, and understanding the events that dictate the rate of formation and growth of polymer particles (see Fig. 1) is difficult. Qualitative understanding can only arise from quantitative measurement of the rate coefficients for each process; these rate coefficients can only rarely be obtained independently, accurately and unambiguously. Until 1980s, this had the effect of providing 'proof' for virtually any proposed kinetic model, due to the large uncertainty and number of adjustable model parameters. Indeed, the first article providing unambiguous *refutation* of a proposed mechanism only appeared in 1988 [3]! Because of this, experimental design for the purpose of elucidating the mechanisms has shifted to minimize the number of adjustable parameters in any given experiment, allowing determination of the mechanism of one process (e.g. radical entry) while controlling other complicating factors (particle formation, initiator concentration, surfactant coverage, etc.). Similarly, the measurement of accurate and unambiguous values of rate coefficients via other means (such as the PLP–SEC method [4–6] for the propagation rate coefficient k_p) has assisted in the reliable and consistent interpretation of kinetic data from emulsion polymerization experiments.

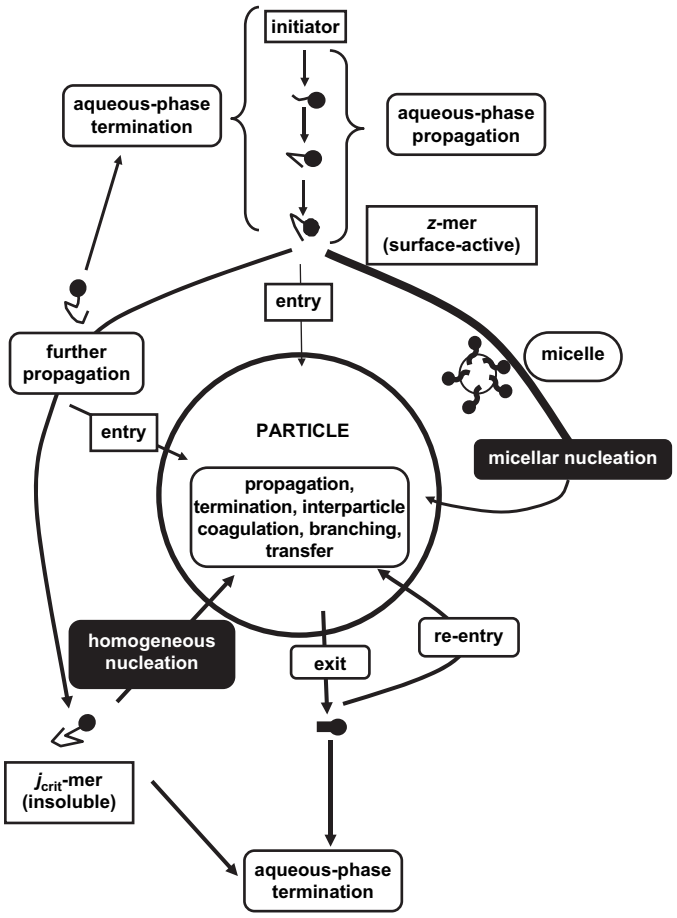

Fig. 1. Full scheme of kinetic processes taking place in a typical emulsion polymerization reaction.

This review focuses on the key mechanistic aspects of emulsion polymerization: radical entry and exit for both electrostatically and electrosterically stabilized particles, particle formation and secondary nucleation, and the termination processes. From the overall rate expression to describe an emulsion polymerization system, various kinetic limits will be described; the applicability of these limits under various conditions allows for a minimal number of model-based assumptions to be made. This not only allows accurate rate parameters to be determined, but also allows for proposed mechanisms to be supported or refuted by appropriately designed experiments.

The focus here is on emulsion homopolymerization, and we concentrate on results with a single monomer, styrene. However, the mechanistic principles are quite general, and are applicable not only to the emulsion polymerization of any single monomer, but also to the copolymerizations. For emulsion copolymerization, the number of parameters required in a model is so large that reliable quantitative *a priori* prediction is probably impossible for the foreseeable future [7]. However, design of new systems and systematic improvements on current ones, needs mechanistic understanding as its basis; the mechanisms here are felt to be generally applicable to any system, *mutatis mutandis*. Moreover, quantitative modelling of complex systems by fixing parameters to fit a limited number of data systems, based on these mechanisms, can be used for semi-quantitative extrapolation and interpolation in related systems.

2. Emulsion polymerization: theoretical overview

A typical batch *ab initio* emulsion polymerization reaction contains three distinct intervals, labeled Intervals I, II and III [8]. Interval I is that where particle formation takes place and monomer droplets, surfactant (and micelles if above the critical micelle concentration, CMC) and precursor particles (a small, colloidally unstable particle that upon further propagational growth, coagulation and adsorption of surfactant will eventually grow to a colloidally stable 'mature' particle) are present. Interval II occurs after the conclusion of the particle

formation period whereby only mature latex particles now exist; the particle number density (N_p, the number of particles per unit volume of the continuous phase) remains constant and the particles grow by propagation in the presence of monomer droplets. As the diffusion of monomer from a droplet to a particle is rapid on the timescale of polymerization, the droplets act as monomer stores that ensure the monomer concentration within a particle is essentially constant (this is in fact an approximation, but solutions to Morton equation [9] describing monomer concentration as a function of particle size show that the saturation concentration is, to a good approximation, constant for all except very small particles; modelling shows that the means used to infer mechanisms from appropriate data discussed in this review are quite insensitive to the small changes predicted by Morton equation [10]). Upon the exhaustion of these monomer droplets, Interval III commences, where the remaining monomer contained within the particles is polymerized. This often, but not always, corresponds to an increase in polymerization rate – above a certain weight fraction of polymer (w_p) within the particle a 'gel' effect exists [11,12] where the effective termination rate is reduced. These three intervals are shown graphically in Fig. 2.

Rate varies as a function of N_p, particle size and initiator concentration ([I]); in the ideal experiment for understanding mechanisms, each of these can be changed independently while all other quantities are kept constant. However, the early attempts used systems where both N_p and size changed together as [I] was changed. The complicated nature of this process means that the rate coefficients for entry and exit could not be determined unambiguously. The method of choice for kinetic experiments for understanding mechanisms is thus seeded experiments that begin in Interval II (by-passing particle formation), wherein N_p and particle size can be controlled independently. It is essential in such experiments that particle formation be avoided during Interval II, since otherwise N_p will change during the experiment, which creates sometimes difficult experimental constraints (e.g. [13]). After the synthesis of a well-defined monodisperse seed latex, further polymerization in the absence of any newly nucleated particles eliminates the complication of polymerization of new particles as well as allowing rates to be obtained with independently varied particle size and particle number.

The value of N_p is obtained from size measurements of the latex using:

$$N_p = \frac{m_p^0}{\frac{4}{3}\pi r_u^3 d_p} \tag{1}$$

where m_p^0 is the mass of the polymer per unit volume of the continuous phase, r_u the volume-average unswollen radius of the seed latex and d_p the density of the polymer.

2.1. The Smith–Ewart equations

The Smith–Ewart equations [14] represent the time evolution of the number of particles containing n radicals (denoted N_n), incorporating the kinetic events that involve the gain and loss of radicals within particles (i.e. radical entry, radical exit, and bimolecular termination). If the population of latex particles is normalized such that

$$\sum_{n=0}^{\infty} N_n = 1 \tag{2}$$

then the average number of radicals per particle (denoted $\overline{n}$, pronounced 'n-bar') is given by:

$$\overline{n} = \sum_{n=1}^{\infty} n N_n \tag{3}$$

Smith and Ewart pointed out that under certain circumstances, it is possible for $\overline{n}$ to have a value of 1/2. In practice, this special value is rarely achieved but only under special conditions [2]; there are many errors in the earlier literature based on the assumption that $\overline{n}$ was *always* 1/2, a fallacy that was only possible to unambiguously prove incorrect with the availability of reliable propagation rate coefficients using pulsed-laser polymerization (PLP–SEC).

Population balance gives the following expression:

$$\frac{dN_n}{dt} = \rho[N_{n-1} - N_n] + k[(n+1)N_{n+1} - nN_n] + c[(n+2)(n+1)N_{n+2} - n(n-1)N_n] \tag{4}$$

where ρ is the pseudo-first-order rate coefficient for entry from the aqueous phase, k is the pseudo-first-order rate coefficient for radical exit (desorption) of a single free radical from a latex particle, and c is the pseudo-first-order rate coefficient for bimolecular termination (again per free radical) between two

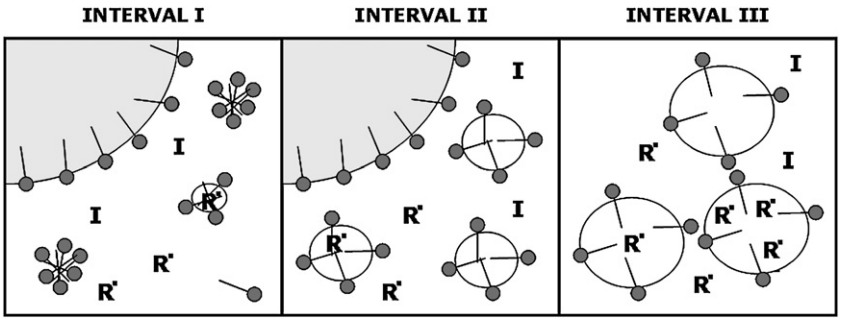

Fig. 2. The three intervals of a typical emulsion polymerization reaction, showing surfactant molecules (—●—), large monomer droplets, micelles (indicated by clusters of surfactant molecules within Interval I), radicals (R•), initiator (I) and surfactant-stabilized latex particles.

free radicals that reside within a single particle. Due to the compartmentalization of radicals within latex particles, bimolecular termination between radicals in different particles need not be considered. The rate coefficients ρ, k and c are dependent on a variety of different variables such as [I], N_p, the particle size, the monomer concentration within the particle phase C_p, or equivalently the weight fraction of polymer w_p, as well as on $\overline{n}$ itself. The microscopic form of these rate coefficients will be given later in this paper.

Considering that polymerization within Interval II is marked by a period of effectively constant polymerization rate (for completeness it should be noted that in systems which obey pseudo-bulk kinetics, such as the polymerization of methyl methacrylate (MMA), there is actually a significant but small acceleration in polymerization rate within Interval II [15]), there is interest in understanding the steady-state behaviour of the solution of Eq. (4), and thereby determining the value for the steady-state value of $\overline{n}$, $\overline{n}_{ss}$. The complete steady-state solution of these equations can be found elsewhere [16,17]. Of particular importance for the determination of mechanistic information from kinetic experiments is the use of various limiting forms of Smith–Ewart equation and the knowledge of the applicability of such limits. Moreover, going beyond the steady-state case enables appropriate time-dependent data to be used, which will be seen to be the means of establishing unambiguous values for the various rate coefficients.

Despite its popularity, there is a fundamental limitation in Eq. (4), because it is implicit that radical loss by termination can be written in terms of a single rate coefficient c. However, it is now well established (e.g. [18]) that the termination rate coefficient depends on the degrees of polymerization ('lengths') of the two terminating chains. Thus in Eq. (4), one must not only have as independent variable n, the number of radicals per particle, but also $N^n_{1,2,\ldots,n}$, the number of these degree of polymerization $1, 2, \ldots, n$ [19]. These equations have not yet been written down in closed form in full generality [19], although as will be seen various limiting forms exist – fortunately sufficient to cover all cases of interest in emulsion polymerizations. The pseudo-first-order rate coefficient c is thus an extremely complex quantity that changes with many variables, including the $N^n_{1,2,\ldots,n}$ that are hidden in Eq. (4). Thus Eq. (4) is generally *invalid*! It is noted that under certain conditions it is possible to use a form of Smith–Ewart equation which takes this chain-length dependence into account [20].

Fortunately, essentially every emulsion polymerization system can to a good approximation be categorized as one or other of two simplifying limits: 'zero-one' and 'pseudo-bulk'. The relevant rate equations are readily solved and render it straightforward to fit experimental data to obtain unambiguous values of rate coefficients. As will be seen, the forms of these limiting equations are rather different from that of Eq. (4).

2.2. The 'zero-one' limit

This limit is a widely applicable one, where the entry of a radical into a particle which already contains a growing chain results in 'instantaneous' termination (to be more precise, termination on a timescale much less than the quantity of interest, such as polymerization rate, i.e. ρ, $k \lll c$). In this limit, intra-particle termination is so fast as not to be rate determining, and the complexities involving c in Eq. (4) disappear. As the name suggests, the 'zero-one' limiting version of Smith–Ewart equation only allows particles to contain zero or one radical at any one time, i.e. $N_n = 0$, $n \geq 2$. As a result only two equations for population balance need to be considered, namely:

$$\frac{dN_0}{dt} = \rho(N_1 - N_0) + kN_1 \tag{5}$$

$$\frac{dN_1}{dt} = \rho(N_0 - N_1) - kN_1 \tag{6}$$

$$\overline{n} = N_1 \tag{7}$$

While these equations are beguilingly simple, they do not take explicit account of the fate of exiting free radicals. Thus, for example, if all exiting radicals have no other fate but to eventually (re-)enter another particle, then the entry rate coefficient depends on the rate of exit, and thus on $\overline{n}$. Taking full account of all the possible fates of an exited radical, as included in Fig. 1, requires a more complicated treatment.

When considering the exit of a radical from a latex particle, it is important to consider the types of radicals that can exit as well as their fate upon exit. In the case of a hydrophobic monomer such as styrene, long polymeric radicals will be insoluble in the aqueous phase. As a result it is assumed in this modelling that monomeric radicals (formed by chain transfer to monomer) will be the only radical species capable of exiting [21] a latex particle due to its 'high' water solubility. Work by McAuliffe [22] on the solubility of a variety of homologous series of hydrocarbon molecules showed that the logarithm of solubility in water is a linear function of the molecular volume of the molecule in question; in the case of styrene at 298 K, a dimeric radical is over 1000 times less soluble in water than a monomeric species. This suggests that the species undergoing exit from a particle will be an uncharged monomeric radical formed via transfer.

The mechanism by which a monomeric radical exits a latex particle is simple diffusion from the particle interior to the aqueous phase. This first-order process is denoted by a rate coefficient k_{dM}; an expression to calculate this rate coefficient can be found in the work of Ugelstad and Hansen [16] and Nomura and Harada [23], derived from considering the microscopic reversibility of desorption and adsorption by using Smoluchowski equation for diffusion-controlled adsorption of a radical into a particle. The resultant expression is:

$$k_{dM} = \frac{3D_w}{r_s^2}\frac{C_w}{C_p} \tag{8}$$

Here D_w is the diffusion coefficient of the monomeric radical in water ($1.3 \times 10^{-9}\ m^2\ s^{-1}$ for styrene at 323 K), C_p the concentration of monomer in the particle phase ($\sim$5.8 M for

styrene at 323 K), r_s the swollen particle radius (related to the unswollen radius r_u and C_p by mass conservation [2]) and C_w the concentration of monomer in the aqueous phase (the saturated value being 4.3 mM for styrene at 323 K [24]). k_{dM} is not the same as the total exit rate coefficient k; a monomeric radial may not desorb (it may instead propagate within the particle), while those that do desorb may undergo homo- or heterotermination, or re-enter another particle. Consideration of these various fates (and determining which fate is the dominant event for the system in question) is needed for the understanding of emulsion polymerization kinetics and will be discussed below.

To allow for the various fates of an exited radical, the added complication of distinguishing between particles containing one monomeric radical (the number of particles satisfying this criteria being denoted N_1^m) and one polymeric radical (the population of which is denoted N_1^p) must be included within the kinetic scheme. This is necessary as an exit (desorption) event can only take place from a particle within the N_1^m population. The evolution equations for a zero-one system are:

$$\frac{dN_0}{dt} = \rho\left(N_1^p + N_1^m - N_0\right) + k_{dM}N_1^m \tag{9}$$

$$\frac{dN_1^m}{dt} = \rho_{re}N_0 - \rho N_1^m - k_{dM}N_1^m + k_{tr}C_pN_1^p - k_p^1C_pN_1^m \tag{10}$$

$$\frac{dN_1^p}{dt} = \rho N_0 - \rho N_1^p - k_{tr}C_pN_1^p + k_p^1C_pN_1^m \tag{11}$$

where k_{tr} is the rate coefficient for radical transfer to monomer, ρ_{re} the pseudo-first-order rate coefficient for re-entry of an exited radical into a particle, k_{tr} the rate coefficient for transfer to monomer and k_p^1 that for propagation of a monomeric radical (which may be significantly greater than that for the equivalent long-chain radical [25]). ρ_{re} can be written as $k_{re}[E^\bullet]$, where $[E^\bullet]$ is the concentration of exited radicals in the aqueous phase and k_{re} the (diffusion-controlled) rate coefficient for entry of a radical into a particle. If the competition between re-entry and aqueous-phase termination is important then:

$$\frac{d[E^\bullet]}{dt} = k_{dM}N_1^m\frac{N_p}{N_A} - k_{re}[E^\bullet]\frac{N_p}{N_A} - 2k_t[E^\bullet][T] \tag{12}$$

where [T] is the total radical concentration within the aqueous phase (it is assumed for simplicity that the chain-length dependence for termination between the oligomeric radicals existing in the aqueous phase can be ignored) and N_A is Avogadro's constant. In general N_1^m is very small and as a result $N_1^p \approx \bar{n}$.

Eqs. (9)–(12) must be solved numerically even in the steady state (Section 5). They contain a number of parameters, ρ, k_{dM} and k_p^1, whose values are hard to determine either from an independent measurement or from a series of rate data, without committing the sin of fitting data containing limited information to a large number of adjustable parameters. However, two sub-limits of the zero-one approximation [21,26] which avoid this problem are widely applicable.

2.2.1. Limit 1 – complete aqueous-phase termination

Limit 1 assumes that all exited radicals undergo either homo- or heterotermination in the aqueous phase and play no further role in the overall polymerization. It is clear from this that the radical-loss mechanism will be first order with respect to $\bar{n}$. Applying the appropriate limits to Eqs. (9)–(11) gives:

$$\frac{d\bar{n}}{dt} = \rho(1 - 2\bar{n}) - k_{ct}\bar{n} \tag{13}$$

where k in this case is denoted k_{ct} (ct = complete termination) and is given by:

$$k_{ct} = k_{tr}C_p\frac{k_{dM}}{k_{dM} + k_p^1C_p} \tag{14}$$

2.2.2. Limit 2 – negligible aqueous-phase termination and complete re-entry

Limit 2 conversely is when it is assumed that all desorbed monomeric radicals re-enter another latex particle rather than terminate in the aqueous phase, i.e. $k_{re}N_p/N_A \gg k_t[T]$. Once re-entered a particle from the N_0 population, this radical can either begin to propagate or desorb once again. The equation describing this limit is given by application of the steady-state approximation to Eq. (10) and substitution into Eq. (11), yielding:

$$\frac{d\bar{n}}{dt} = \rho(1 - 2\bar{n}) - 2k_{tr}C_p\left(\frac{k_{dM}\bar{n}}{k_{dM}\bar{n} + k_p^1C_p}\right)\bar{n} \tag{15}$$

Even further subdivisions of this limit can be established by considering the relative magnitudes of $k_p^1C_p$ and $k_{dM}\bar{n}$. If the monomeric radical will most likely propagate (i.e. $k_p^1C_p \gg k_{dM}\bar{n}$) then Eq. (15) reduces to:

$$\frac{d\bar{n}}{dt} = \rho(1 - 2\bar{n}) - 2\frac{k_{tr}k_{dM}}{k_p^1}\bar{n}^2 \equiv \rho(1 - 2\bar{n}) - 2k_{cr}\bar{n}^2 \tag{16}$$

Eq. (16) is known as the Limit 2a expression; the radical-loss term is of second order with respect to $\bar{n}$ (as two particles are required for a monomeric radical to be destroyed). The exit rate coefficient k in this case is denoted k_{cr} (cr = complete re-entry) and is given by:

$$k_{cr} = \frac{k_{tr}k_{dM}}{k_p^1} \tag{17}$$

Limit 2a is accepted as the kinetic regime that governs most styrene emulsion polymerizations [21,27], as the relatively large product $k_p^1C_p$ ensures that a re-entered radical will propagate before further desorption. The converse case where desorption is more likely than further propagation is known as Limit 2b and is not widely applicable.

2.3. The pseudo-bulk kinetic limit

Discussion so far has been restricted to emulsion polymerization systems in which intra-particle termination is so fast as not to be rate determining. While valid for sufficiently small particles [27], one must also consider those systems where this approximation breaks down. As stated, because of chain-length-dependent kinetics, the complete kinetic equations describing this (the full generalization of Smith–Ewart equations) cannot be written in closed form (although some limited solutions for this exist, e.g. in the so-called 'zero-one-two' case [20]). However, a convenient and widely applicable limit is when it is assumed that compartmentalization of radicals into particles has no effect on the kinetic equations (although the actual rate coefficients therein may be affected). This can happen in two separate cases or a combination of both: when (i) exited free radicals never terminate in the aqueous phase and jump (re-enter and re-exit) from particle to particle until eventually propagating and/or (ii) the value of $\overline{n}$ is sufficiently high that the intra-particle kinetics are the same as in a bulk system. Explicit and easily implemented criteria for determining whether a given system will fit this limit or the zero-one limit have been presented [28,29]. It is important to be aware that for certain monomers such as methyl methacrylate [30] and butyl acrylate [28], quite small particles can obey pseudo-bulk kinetics, and the steady-state value of $\overline{n}$ can be quite low, indeed significantly less than 1/2. As explained in Refs. [30,28], this is because a monomer with a sufficiently high propagation rate coefficient can lead to a situation where any new radical in a particle (formed by transfer or arriving by entry from the aqueous phase) will propagate so quickly that it will quickly grow long, in which case its termination rate coefficient with any other radical is reduced, because termination is diffusion-controlled and thus slower for larger radicals; monomers with sufficiently high k_p can thus have more than one radical per particle, even for relatively small particles. This is an explicit effect of chain-length-dependent termination.

When the effect of compartmentalization of radicals is unimportant, one can treat the kinetics as those of a bulk system, expressed in terms of a per-particle rate. That is, instead of the bulk radical concentration [R], one uses

$$\overline{n} = \frac{[\mathrm{R}]}{N_\mathrm{A} V_\mathrm{s}} \tag{18}$$

where V_s is the swollen volume of a particle. That is, one no longer needs to consider each particle as having a different reaction scheme, depending on how many radicals it contains. Thus one has:

$$\frac{\mathrm{d}\overline{n}}{\mathrm{d}t} = \rho - k\overline{n} - 2\langle c\rangle \overline{n}^2 \tag{19}$$

where the entry rate coefficient includes contributions from re-entry of exited radicals, k is the overall first-order rate coefficient for exit, and the quantity $\langle c\rangle$ is the *chain-length-averaged* value of the termination rate coefficient:

$$\langle c\rangle = \frac{\langle k_\mathrm{t}\rangle}{N_\mathrm{A} V_\mathrm{s}}; \quad \langle k_\mathrm{t}\rangle = \frac{\sum_i \sum_j k_\mathrm{t}^{ij} R_i R_j}{\left(\sum_i R_i\right)^2} \tag{20}$$

Here k_t^{ij} is the termination rate coefficient between radicals of degrees of polymerization i and j, and R_i is the concentration of radicals of degree of polymerization i. The individual k_t^{ij} is both chain-length and conversion dependent; shorter chains, due to their faster diffusion, undergo termination more rapidly than long polymeric radicals. R_i is obtained by solving the appropriate population balance equations, which for simplicity are presented below only for $i \geq 2$:

$$\frac{\mathrm{d}R_i}{\mathrm{d}t} = \rho\delta_{iz} + \left(k_\mathrm{p}^{i-1} R_{i-1} - k_\mathrm{p}^i R_i\right) C_\mathrm{p} - k_\mathrm{tr} C_\mathrm{p} R_i - 2R_i \sum_{j=1}^{\infty} \frac{k_\mathrm{t}^{ij}}{N_\mathrm{A} V_\mathrm{s}} R_j, \quad i \geq 2 \tag{21}$$

(see Ref. [19] for the general expressions), $\delta_{ij} = 0$ for $i \neq j$, and $\delta_{ij} = 1$ for $i = j$, and z is the degree of polymerization of entering radicals (for notational simplicity the differences between entering radicals derived directly from initiation and re-entry are disregarded). These equations are readily solved numerically [19] in the steady state for R_i, which is an excellent approximation even in systems where the overall rate is changing rapidly [31].

The nature of the termination reaction is such that the value of $\langle c\rangle$ may change dramatically as a function of conversion (as the weight fraction of polymer w_p within the particle will change), in particular as the system goes through the gel regime.

In the common case where all exiting radicals re-enter another particle, the overall entry rate coefficient ρ is given by $\rho = \rho_{\mathrm{init}} + k\overline{n}$, where ρ_{init} is the component of the entry rate coefficient arising directly from radicals generated in the water phase entering into particles. In this case Eq. (19) simplifies to

$$\frac{\mathrm{d}\overline{n}}{\mathrm{d}t} = \rho_{\mathrm{init}} - 2\langle c\rangle \overline{n}^2 \tag{22}$$

An analytic solution to the pseudo-bulk equation can only be found if ρ and $\langle c\rangle$ are constant over the timescale of interest (e.g. during the rapid relaxation of a system after removal from a γ-radiolysis source – see Section 3.2) [15,30]:

$$\overline{n} = \overline{n}_\mathrm{f} \frac{Q\exp(2\delta t) - 1}{Q\exp(2\delta t) + 1}; \quad Q = \left(\overline{n}_\mathrm{f} + \overline{n}_\mathrm{i}\right) / \left(\overline{n}_\mathrm{f} - \overline{n}_\mathrm{i}\right), \quad \delta = 2\langle c\rangle \overline{n}_\mathrm{f}, \tag{23}$$

where $\overline{n}_\mathrm{i}$ and $\overline{n}_\mathrm{f}$ denote the initial and final steady-state values of $\overline{n}$, respectively. It is important to also consider that the value of k_t measured from experiment is not a single value but actually an average, $\langle k_t\rangle$, as the rate of termination between two chains is heavily chain-length dependent [2,32]. The individual k_t^{ij} is a function of both the diffusion coefficients of the

species in question and the radius of their interaction. Further discussion of the radical termination mechanism will be presented later in this review.

2.4. The rate of an emulsion polymerization

The rate of a polymerization is normally defined as the rate of consumption of monomer:

$$\frac{d[M]}{dt} = -k_p[M][R] \tag{24}$$

where [M] is the concentration of the monomer and [R] the total radical concentration. In an emulsion where the polymerization only takes place within the particle interior, [M] is replaced by C_p; the total radical concentration is $\overline{n}N_p/N_A$. As it is experimentally convenient to measure the fractional conversion of monomer into polymer (denoted x, where $0 \leq x \leq 1$), a change in variable is made and the rate of fractional conversion is now considered, giving:

$$\frac{dx}{dt} = \frac{k_p C_p N_p}{n_M^0 N_A}\overline{n} \tag{25}$$

where n_M^0 is the initial number of moles of monomer per unit volume of the continuous phase (all other parameters as defined previously). Eq. (25) shows that $\overline{n}$, including its time dependence, can be obtained experimentally via accurate monitoring of the polymerization rate. The application of this will be discussed below.

3. Emulsion polymerization: experimental techniques

3.1. Synthesis of seed latexes

Seeded experiments are used to avoid the complications of the particle formation mechanism and its kinetics, i.e. a pre-synthesized latex that is well-characterized and is then polymerized further after swelling with monomer. Only experiments in which no secondary particle formation (new nucleation) occurs are useful for kinetic analysis to obtain unambiguous values of particle-growth rate coefficients. As kinetic parameters such as k_{dM} are often functions of particle size, an ideal seed latex is one that has a narrow particle size distribution (PSD). This can be achieved by synthesizing the seed at a relatively high temperature [2], which results in a higher radical flux that shortens the particle formation time, followed by a long period of growth without further particle formation. A typical electrostatically stabilized seed latex recipe (polymerization conducted at 363 K with conventional free-radical initiation) is given in Table 1.

The recipe in Table 1 produces monodisperse polystyrene latex particles of radius ~30 nm after 1 h reaction time. All ingredients should be purified beforehand; monomers such as styrene should be distilled under vacuum to remove impurities and polymerization inhibitors. The resultant latex should be dialyzed for approximately 1 week with regular changes of distilled water to remove residual surfactant, monomer and aqueous-phase oligomers. The particle size (and PSD) is then usually confirmed via transmission electron microscopy (TEM) or a separation technique that separates particles on the basis of size such as hydrodynamic chromatography.

Table 1
Typical laboratory recipe for the synthesis of an electrostatically stabilized seed latex

Ingredient	Quantity (g)
Monomer (styrene)	300
Water	625
Initiator (potassium persulfate)	1
Buffer (sodium hydrogen carbonate)	1
Surfactant (Aerosol MA 80)	10.5

The synthesis of well-characterized electrosterically stabilized latexes presents a more difficult problem. Electrosteric stabilization (using ionizable water-soluble polymers grafted to the particle surface to impart colloidal stability) is a common technique in the synthesis of industrial polymers for use in surface coatings and adhesives. A typical recipe involves a variation of that given in Table 1, wherein a water-soluble co-monomer is added. While easy to synthesize, characterization of the 'hairy layer' on the particle surface is extremely complicated. Due to the very high (and variable under different conditions) propagation rate coefficient of acrylic acid [33,34]), the molecular weight distribution of the poly(acrylic acid) blocks on the surface is likely to be very broad and polydisperse, and characterization of the size of this layer by scattering technique such as small-angle neutron scattering (SANS) cannot be unambiguously interpreted to yield even a moderately precise result [35].

A new route to the synthesis of well-defined electrosteric latexes has recently been developed through the advent of successful controlled-radical polymerization in emulsion [36–38], in particular the reversible addition-fragmentation chain transfer (RAFT) technique. This results in small particles with very narrow size distributions. RAFT is well established as a robust means to synthesize polymers of low polydispersity while retaining their 'living' nature [39]. However, until recently [40] the use of RAFT within emulsion had proven impossible. Ferguson et al. [37,38] developed the first electrosterically stabilized emulsion under complete RAFT control through the use of an amphipathic RAFT agent that allowed the synthesis of relatively monodisperse hydrophilic block in water as the first step. Subsequent starved-feed addition of a hydrophobic monomer into the aqueous phase eventually results in self-assembly of diblock copolymer chains (the beginning of particle formation), after which the particles continue to grow to any size. The reaction scheme for this is shown in Fig. 3.

3.2. Measurement of rate

Determination of accurate rate coefficients requires accurate data for the fractional conversion of monomer into polymer as a function of time. This can be obtained with sufficient accuracy using for example calorimetry or dilatometry

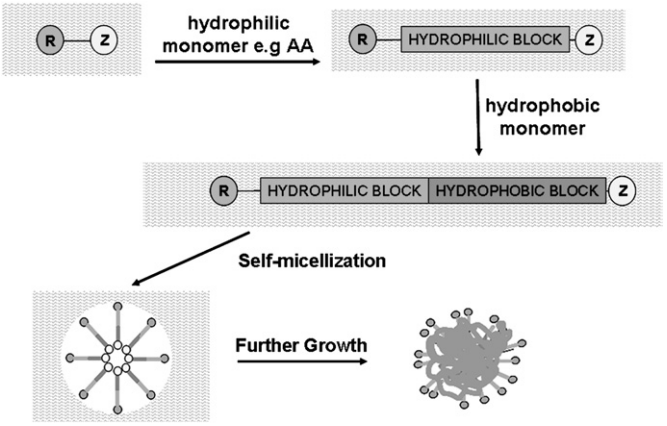

Fig. 3. Synthesis of an electrosterically stabilized seed latex using RAFT.

(other useful techniques such as on-line Raman spectroscopy [41] will not be discussed here).

Dilatometric works on the premise that the density of a polymer is slightly larger than the density of its component monomer, and as a result the polymerization medium shrinks as a function of time. Using a polymerization vessel with a narrow capillary in the top, this contraction can be monitored accurately by measuring the change in meniscus height as a function of time by an automated tracking device. It is the most precise technique for measuring the time dependence of conversion, but has limitations such as the need for very precise temperature control and for assuming ideal mixing (or correcting for this by calibration, e.g. in systems such as dienes [42]). Dilatometry cannot be readily used either in copolymerizations or in systems wherein monomer or other ingredients are fed in during the reaction. Calorimetry does not suffer from these drawbacks [43–51] but particular care needs to be taken to obtain data of sufficient accuracy for reliable mechanistic inferences [51]. A typical conversion–time curve is shown in Fig. 4.

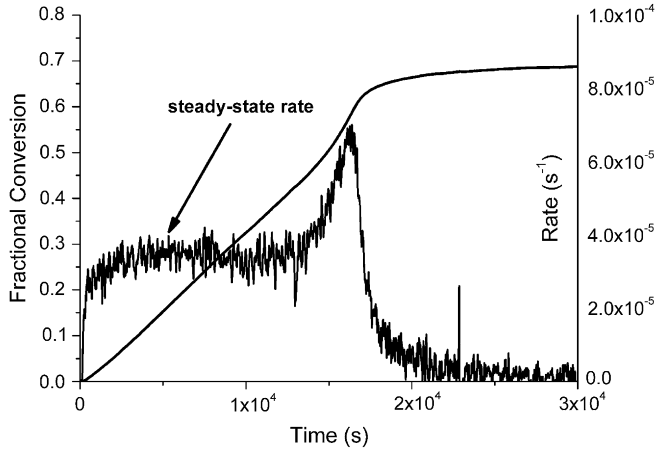

Fig. 4. Conversion–time data and rate (as the numerical derivative of x, which shows noise) obtained from dilatometric study of an emulsion polymerization of styrene. Experiment performed at 323 K using a preformed poly(styrene) seed ($N_p = 3 \times 10^{17}$ L^{-1}, unswollen radius = 25 nm, 10 g latex used), KPS as initiator (concentration 1 mM), purified styrene as monomer added to ensure saturation of the particle phase; reaction vessel was a 30 mL jacketed dilatometric vessel kept at a regulated temperature by an external water bath.

An experiment that allows direct access to the radical-loss mechanism is the use of γ-radiolysis dilatometry in 'relaxation mode.' γ-Radiation initiates an emulsion polymerization through the formation of $^{\bullet}$OH and high energy electrons that soon become protonated [52]. While initiation in these systems is complex, the power of this technique is the fact that unlike chemical initiation, the radical flux in these systems can be 'switched off' by removing the sample from the radiation source and observing a decrease in the polymerization rate; the radical-loss kinetics from this rate reduction are independent of the complexities of the radiolytic initiation events. The penetrating power of γ-rays enables uniform initiation over many centimeters in an opaque latex (which cannot be achieved by photoinitiation with UV radiation). The dilatometric set-up can be raised and lowered into a ^{60}Co γ source (see Fig. 5). Upon removal of the sample from the radiation source, the polymerization rate slows over time until it reaches a new 'out-of-source' steady-state rate (which is not necessarily zero [53], for reasons that will be discussed later). Monitoring of the change in rate as a function of time gives direct access to the exit rate coefficient k in a system following zero-one kinetics [53], or to $\langle k_t \rangle$ in a system following pseudo-bulk kinetics [30], as the only way that the polymerization rate is decreased is through radical loss from the polymerization locus. Re-introducing the sample into the radiation source should lead to a return to the original in-source rate (see Fig. 6).

3.3. Determination of kinetic parameters and rate coefficients

For seeded experiments where the N_p of the latex and the initial amount of monomer (n_M^0) are known (as well as an accurate value of the propagation rate coefficient k_p for the monomer in question and conditions where the monomer concentration within the particles, C_p, is essentially constant), Eq. (25) shows that the polymerization rate is directly proportional to $\overline{n}$, i.e.

$$\frac{dx}{dt} = A\overline{n} \tag{26}$$

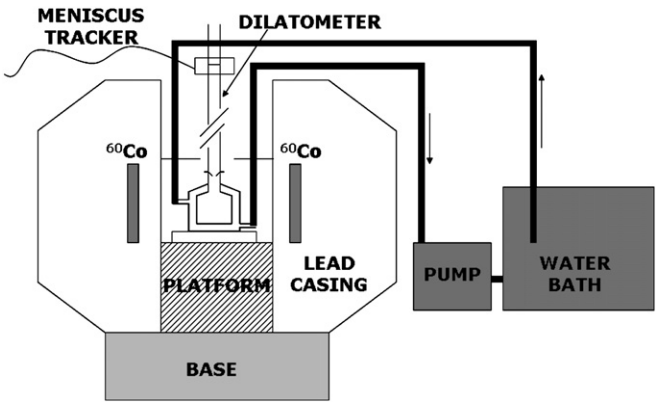

Fig. 5. γ-Radiolysis dilatometry experimental set-up.

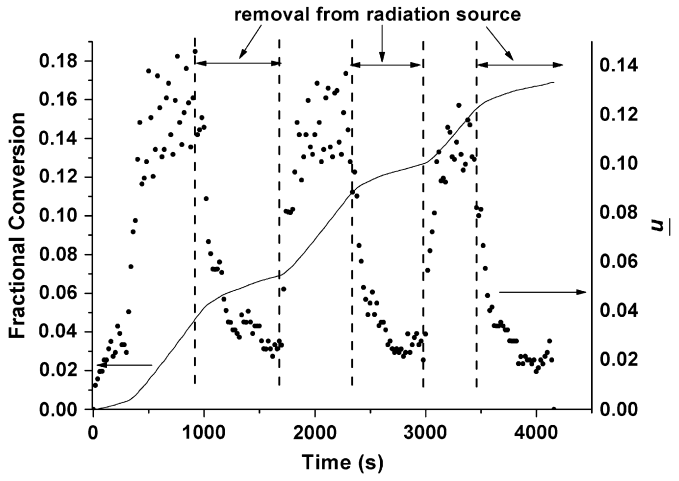

Fig. 6. Typical conversion–time data, and time dependence of $\overline{n}$ from numerical differentiation of the conversion, from a γ-radiolysis dilatometry experiment with multiple removals and insertions from the γ source. The time periods when the reactor vessel was removed from the source are indicated.

where A is the collection of constants in Eq. (25). This relation gives the time evolution of $\overline{n}$ and, if there is a significant region of constant rate, of its steady-state value $\overline{n}_{ss}$. The absence of any secondary nucleation must be confirmed via TEM or a chromatographic technique; light scattering measurement of average particle size is inadequate for this purpose, because light scattering is biased towards larger particles, whereas newly formed particles are small and therefore often undetectable by this method.

The polymerization rate is often constant within Interval II in a zero-one system, as evidenced by $x(t)$ being linear for a substantial period. Assuming constant values of ρ and k, the appropriate rate equation for the time evolution of $\overline{n}$ can be integrated to arrive at an expression that relates the nature of the conversion–time curve to the rate coefficients in question. For example, assuming no re-entry of exited radicals (Eq. (13)), one has:

$$\overline{n} = \frac{\rho}{2\rho + k} + \left(\overline{n}_0 - \frac{\rho}{2\rho + k}\right) e^{-(2\rho + k)t} \tag{27}$$

where $\overline{n}_0$ is the initial value of $\overline{n}$ at $t = 0$. Combination of Eqs. (26) and (27) and further integration yields:

$$x(t) - x_0 = \frac{A}{2\rho + k}\left\{\rho t + \left(\overline{n}_0 - \frac{\rho}{2\rho + k}\right)\left(1 - e^{-(2\rho + k)t}\right)\right\} \tag{28}$$

where x_0 is the fractional conversion at $t = 0$. At the long-time limit, Eq. (28) reduces to a linear expression as a function of time, i.e. $x(t) - x_0 = a + bt$ where a and b are the intercept and slope of the linear region of the conversion–time plot. Thus accurate measurement of the slope and intercept can be used to calculate ρ and k – the 'slope and intercept' method. The values for the two rate coefficients are:

$$\rho = \frac{b}{a}\left(\overline{n}_0 - \frac{b}{A}\right) \tag{29}$$

$$k = \left(\frac{A}{a} - 2\frac{b}{a}\right)\left(\overline{n}_0 - \frac{b}{A}\right) \tag{30}$$

This technique demonstrates that both rate coefficients can be obtained with a minimum of model-based assumptions.

The assumption of re-entry of exited radicals (Limit 2a, Eq. (16)) leads to an equivalent conversion–time function:

$$x(t) - x_0 = \frac{A(p - \lambda)}{\gamma} \ln\left\{\frac{1 - \delta \exp(-\gamma t)}{1 - \delta}\right\} + Apt \tag{31}$$

$$p = \frac{2\rho - \gamma}{-4k};\ \lambda = \frac{2\rho + \gamma}{-4k};\ \gamma^2 = 4\rho(\rho + 4k);\ \delta = \frac{p - \overline{n}_0}{\lambda - \overline{n}_0} \tag{32}$$

Knowledge of the slope (a) and intercept (b) from the Interval II steady-state period allows calculation of ρ and k from Eq. (31), namely:

$$k = A\frac{\ln F}{2a},\ \rho = Gk \tag{33}$$

$$G = \frac{2b^2}{A(A - 2b)},\ F = \frac{1}{2} + \frac{G + 2\overline{n}_0}{4G(G + 2)^{0.5}} \tag{34}$$

While the slope and intercept method is easily implemented to determine ρ and k, it can be prone to significant error. The biggest difficulty is that an accurate value of the intercept is not easy to find, as small perturbations in the early stages of the polymerization (i.e. residual oxygen acting as an inhibitor, difficulty in determining the true starting time) can greatly affect the value of the intercept. The long-term slope, however, can be easily and accurately found, so ideally a second, independent technique should be employed to determine one of the rate coefficients in question.

The ideal technique to do this is to utilize γ-radiolysis dilatometry in relaxation mode, for direct access to k. This can be done by fitting the appropriate time evolution equation for $\overline{n}(t)$ (depending on whether the system obeys Limit 1 or Limit 2a kinetics) to the non-steady-state period where the reaction rate is decreasing (as the sample has been removed from the radiation source). An appropriate data fitting technique yields k (as well as the 'thermal' or 'spontaneous' entry rate coefficient ρ_{spont} [54], as the out-of-source rate is often non-zero in many emulsion systems). Once a k value has been established by this means, a value for ρ can be determined from the steady-state rate in a chemically initiated system, as:

$$\rho = \frac{k_{ct}\overline{n}_{ss}}{1 - 2\overline{n}_{ss}}(\text{Limit 1});\ \rho = \frac{2k_{cr}\overline{n}_{ss}^2}{1 - 2\overline{n}_{ss}}(\text{Limit 2a}) \tag{35}$$

and $\overline{n}_{ss}$ is found from the slope of the linear (long-time) region of the conversion–time curve. This technique, using two independent experimental processes, yields rate coefficients of much greater accuracy, ensuring the best means to support or refute potential mechanisms.

4. Radical exit

4.1. Electrostatically stabilized emulsion systems – the fate of an exited radical

As mentioned, radical exit can only occur via monomeric radicals generated by transfer, as they have the highest solubility in the aqueous phase [21]. The rate-determining steps are formation of these radicals by transfer to monomer, removal of these radicals by propagation to a higher degree of polymerization, and diffusion of the radical away from these particles through the water phase. The rate coefficient for desorption of a monomeric radical (k_{dM}, Eq. (8)) has an inverse-square dependence on r_s; the total exit rate coefficient k also allows for the likelihood of desorption relative to other fates within the particle (such as further propagation).

Once a radical has exited, the importance of its fate in the aqueous phase is paramount to truly understand the kinetics in emulsion polymerization systems. The exited radical E$^\bullet$ can either propagate in the aqueous phase, terminate with another radical (note that an exited, uncharged monomeric radical is chemically distinct from an initiator-derived oligomer, most likely bearing a charge) or re-enter into another particle. The concentration of particles and of radicals that can potentially terminate an exited radical (such as initiator-derived radicals) must be taken into account in finding the probabilities of various fates for an exited species. In the pioneering work of Smith and Ewart [14], some assumptions were made that methods developed subsequently have shown to be incorrect, including that radical loss was first order with respect to $\bar{n}$ (Eq. (13)): however, for many systems, re-entry cannot be neglected.

A breakthrough came when Lansdowne et al. [53] measured radical loss using γ-radiolysis dilatometry experiments in relaxation mode. These loss data can be processed assuming both first- and second-order loss kinetics; it was seen that when the 'thermal' or spontaneous entry rate of radicals is considered (see Section 5), loss in styrene systems follows second-order kinetics. This was further supported in the work of Morrison et al. [27], where various techniques (such as the approach to steady state in chemical and γ-initiated experiments) showed that the most likely fate for a styrene monomeric radical is to exit, re-enter and either propagate or terminate (Limit 2a, Eq. (16)), as shown in Fig. 7. The modelling of Casey et al. [21] also showed that unless the particle number (N_p) is extraordinarily low ($<10^{13}$ L^{-1}), re-entry will be the dominant fate over termination by several orders of magnitude. The likelihood of various fates are shown in Fig. 8. Such calculations are easily done for most monomers, with the fact that the rates of the possible fates differ by orders of magnitude rendering the conclusions from such calculations insensitive to precise rate coefficient values.

As shown in Fig. 9, data for styrene seeded emulsion polymerizations in electrostatically stabilized latexes [27,55] are well fitted by this model, as described by Eqs. (16) and (8). In this fitting, parameters were chosen as follows: that for k_p from PLP studies [6], k_{tr} from molecular weight distribution

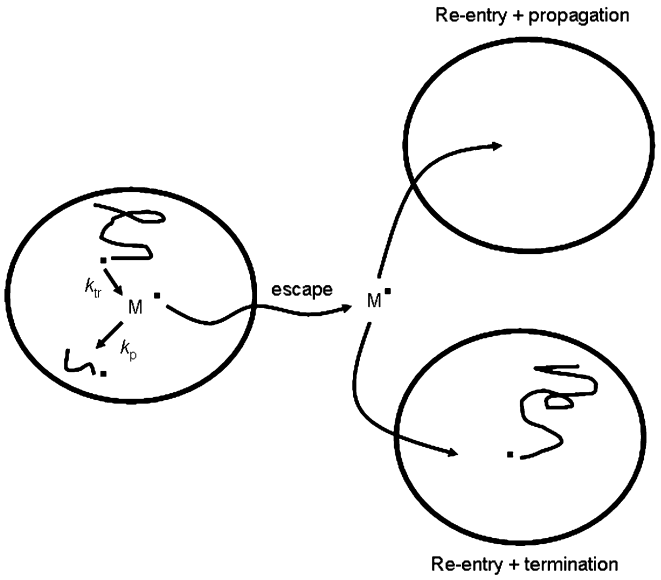

Fig. 7. Radical loss via the 'Limit 2a' mechanism – desorption, followed by re-entry.

data [56], and k_p^1, the rate coefficient for propagation of a monomeric radical, to be 2–4 times the long-chain value (k_p). From basic quantum mechanical and transition state theory arguments (including very accurate calculations) [25] it is expected that the propagation rate coefficient of a monomeric radical will be several times larger than the long-chain limit (normally considered between 2 and 10 times larger [57]). Unfortunately no reliable experimental values of k_p^1 exist, and given the degree of experimental scatter in the exit rate coefficient data, slightly different values of k_p^1 can give an adequate fit to the data. Nonetheless, an inverse-square dependence on the particle radius exists with respect to the rate coefficient of radical exit. While the value of k_p^1 can be treated as an adjustable parameter, it cannot be adjusted outside the range indicated by fundamental theory.

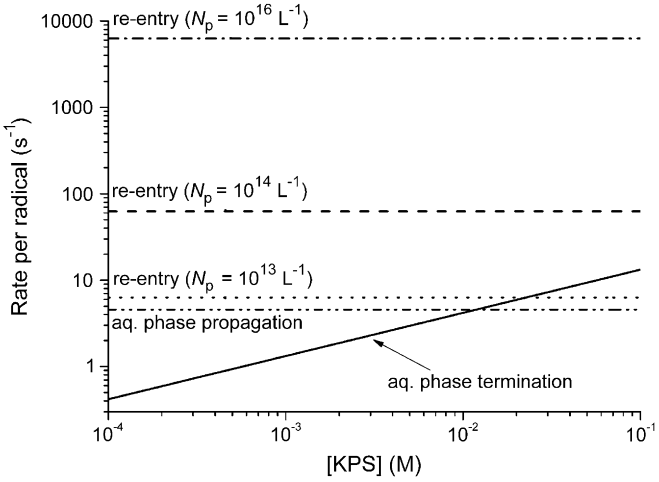

Fig. 8. Rates of the various kinetic fates of an exited monomeric radical in a styrene emulsion system at 323 K as a function of initiator (persulfate) concentration, for particle size $r_s = 50$ nm.

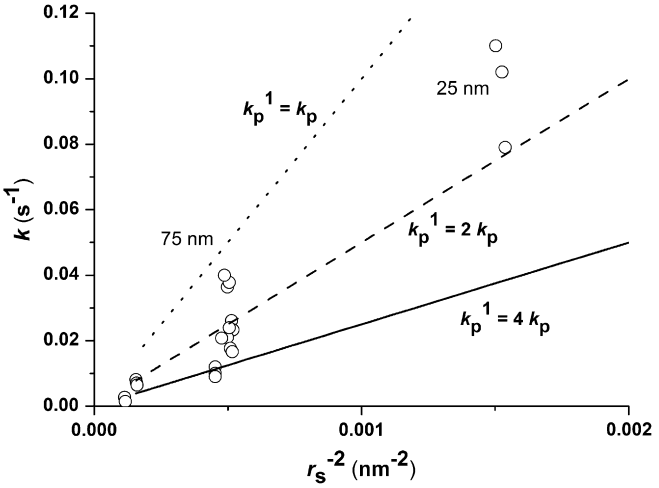

Fig. 9. Experimental data [27,55] for exit rate coefficients (points) for seeded emulsion polymerization of styrene in electrostatically stabilized latex particles over a range of swollen particle radii (r_s) and model predictions, as described in the text.

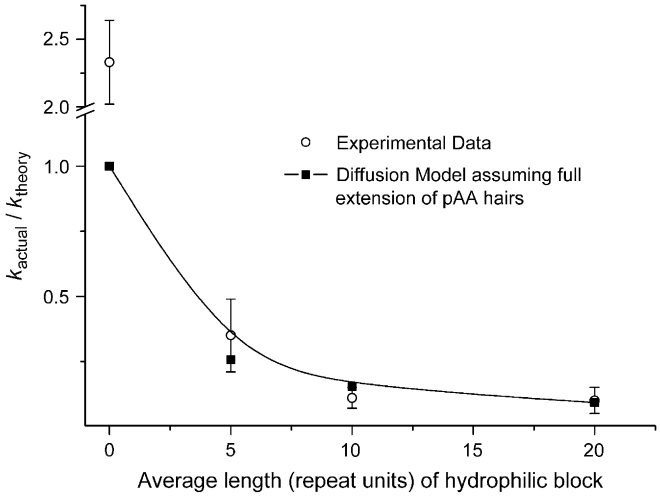

Fig. 10. Variation of the exit rate coefficient ratio $k_{experimental}$:k_{theory} as a function of poly(AA) hair length in electrosterically stabilized systems and comparison with the kinetic model given by Eqs. (16) and (17) (solid line).

4.2. Electrosterically stabilized emulsion systems

Work on radical exit using seeded dilatometric experiments on poly(AA)-stabilized styrene latexes [13,58] demonstrated a significant reduction in k relative to an equivalent electrostatically stabilized latexes under various conditions. The reduction in k was a function of the density of the poly(AA) coverage on the particle surface, was pH dependent and was complicated by the issue of secondary nucleation. However, the observed decrease, under all conditions, was consistent with a descrease in the desorption rate of the exiting monomeric radical in the presence of a layer of polymer on the particle surface.

This postulate was rigorously tested by the present authors [59] in the first use of electrosterically stabilized emulsions made by a controlled-radical process, where the length of the 'hairy layer' was controlled by synthesizing latexes with different lengths of poly(AA) on the particle surface. Again a significantly lower value of k was observed in these latexes (see Fig. 10), with the value of k decreasing as a function of 'hair' length. This was successfully modeled by modification of Smoluchowski equation for diffusion-controlled reactions to account for a region of slow diffusion around the particle surface, i.e. the diffusion coefficient within the hairy layer is significantly lower than that of the aqueous phase ($D_h \ll D_w$). The results were also in agreement with other established kinetic models for radical desorption in such systems [60].

While this assumption provided an explanation for the reduced exit rate coefficient in these systems, the complementary results for radical entry (Section 5.5) seemed to be in conflict with this explanation. Maintaining the assumption that styrene obeys Limit 2a kinetics in these electrosterically stabilized latexes that satisfy the zero-one criteria, entry rate coefficients were calculated using k_{cr} (from γ-relaxation experiments) and the $\overline{n}_{ss}$ value from chemically initiated experiments using Eq. (35); it was seen [61] that the values of ρ so obtained were impossibly small, well below the expected spontaneous entry rate coefficient ρ_{spont} (in many systems, in the absence of any radical flux from initiator the polymerization rate is non-zero due to what is dubbed 'spontaneous polymerization'; typically this is only a small contribution to the overall entry rate coefficient. This topic is discussed in more detail in Section 5). On the other hand, using Limit 1 kinetics (Eq. (13)) to calculate ρ from the chemically initiated steady-state $\overline{n}_{ss}$ values gave excellent agreement with Maxwell–Morrison 'control by aqueous-phase growth [62]' entry mechanism (Section 5.2). This suggested that termination in either the aqueous or surface phases, rather than re-entry, was the dominant fate of exited radicals in electrosterically stabilized systems, meaning that the loss mechanism in these systems had to be re-considered.

Under most conditions, re-entry is calculated to be significantly more important than termination in styrene systems (Fig. 8), and thus these results were difficult to rationalize. Given that these particles are, in essence, polystyrene particles with a layer of poly(AA) grafted on the surface, an extra loss mechanism due to interaction of an exiting radical with the poly(AA) hairy layer was put forward. The system is such that mid-chain radicals (MCRs) can readily form on the poly(AA) hairy layer. This could be through transfer/H-atom abstraction (shown to be possible in bulk styrene polymerizations in the presence of poly(AA) [61]), as well as through grafting [63] and chain transfer to polymer that is dominant within the acrylate family [64]. This MCR is slow to propagate but quick to terminate, and thus provides a new loss mechanism: termination with a mid-chain radical. These additional mechanisms (see Fig. 11) were added to the standard emulsion polymerization kinetic equations (Eqs. (9)–(11)) to give an extended kinetic model [61,65] to rationalize the experimentally observed results in these systems. Modelling was performed with the number of stabilizing chains per particle held constant while the particle size was increased; the results demonstrated that for very small particles (such as the ones created by the

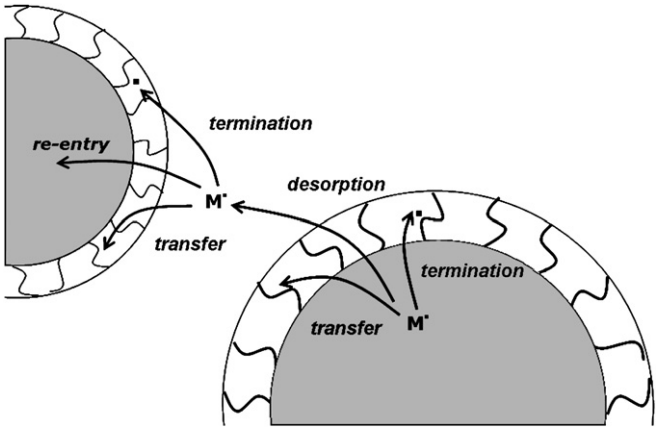

Fig. 11. Additional loss terms (transfer and termination) included in the radical-loss mechanism for electrosterically stabilized emulsion systems.

RAFT-in-emulsion method), the first-order loss mechanism (Limit 1) is dominant, as the hairy layer is densely packed (assuming that the chains are fully extended, the volume fraction of acrylic acid in the hairy layer of a particle of radius 20 nm stabilized by the pentameric diblock is 7%, assuming a realistic value of 250 stabilizing chains per particle; corresponding to local concentration of AA units within the hairy layer of ~1 M) and an exiting radical is more likely to encounter a transfer/termination site rather than desorb. For significantly larger particles but with the same total number of stabilizing hairs per particle (meaning the average surface area per stabilizing chain and local acrylic acid concentration significantly decreases), Limit 2a kinetics are dominant: desorption (and hence re-entry) is the dominant fate of a monomeric species. The magnitude of the relative loss terms as a function of particle size is shown in Fig. 12. Results demonstrated that this is not the length of the stabilizing chain on the surface that is of primary importance, but the local polymer concentration. In the future it would be interesting to consider the behaviour of these systems as the degree of ionization of the acid monomer on the surface is varied, which will most likely change the orientation of the stabilizing chains and affect the available surface area and local polymer density.

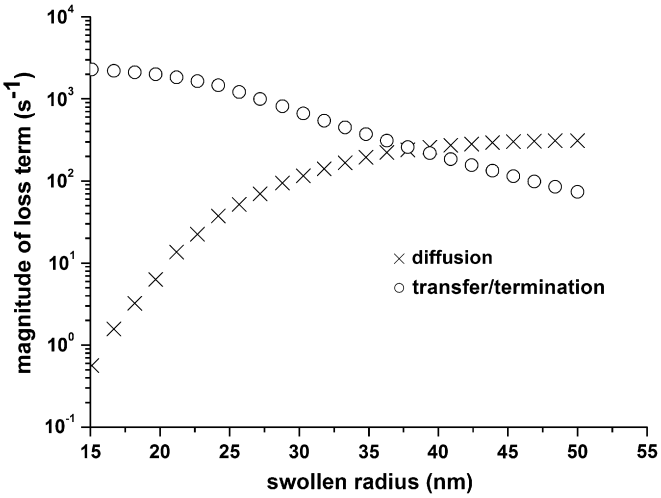

Fig. 12. Transfer/termination versus desorption as a function of particle size in the electrosterically stabilized emulsion kinetic model; model parameters [persulfate] = 1 mM, latex solids 10%, latex stabilized by pAA chains of average degree polymerization = 5 (250 chains per particle).

This kinetic model is for systems with a hydrophilic polymer on the surface that can undergo a hydrogen-atom abstraction reaction; this includes stabilizers containing (co-)polymers of acrylic acid [61,65] or ethylene oxide [66]. These are common in industry.

5. Radical entry

5.1. Previously postulated entry mechanisms

The radical entry mechanism has been, over time, a much disputed components of the entire mechanistic picture that governs emulsion polymerization kinetics. This has been due in part to the inability to measure accurate entry rate coefficients in order to refute potential mechanisms, as well as minimizing the number of adjustable parameters to ensure that a model cannot be 'tweaked' to fit experimental data.

As the majority of initiators used in emulsion polymerization systems is water-soluble, while nearly the entire polymerization takes place in the particle interior, there must be an entry mechanism whereby radicals can cross from the aqueous phase into the particle. The original supposition that all radicals formed by fragmentation of initiator eventually enter a particle [14] was proven to be incorrect in the work from the author's laboratory [30,67,68] demonstrating that radical entry efficiencies (the fraction of initiator-derived radicals that do enter a particle) could be observed experimentally that were much less than unity, indicating significant aqueous-phase termination prior to entry. Many models have been put forward to explain the entry mechanism, but all but one have been refuted in some manner [3].

The first attempt to elaborate on the entry mechanism was the 'diffusive entry model', which assumed that the rate-determining step for entry was the simple diffusion of an entering radical to the particle surface [69]. This, however, yielded values of k_e (the second-order rate coefficient for entry) that were orders of magnitude larger than experiment. Yesileeva [70] suggested that the rate-determining step in the radical entry process might involve requiring the desorption of a surfactant molecule off the particle surface to allow a radical to enter into the particle interior; this mechanism, however, would suggest that the entry rate coefficient would be a function of surface coverage on the particle surface. This inference was refuted experimentally [3]; this was the first time that it was possible to unambiguously refute a postulated mechanism in emulsion polymerization systems.

The work of Penboss et al. [71] in the area of seeded emulsion polymerization of styrene (initiated with persulfate) suggested that the entry process might be either a diffusion-controlled event dependent on surfactant displacement (later disproved by the just-cited data [3]), or that the entering species is of colloidal dimensions (with a degree of polymerization of the order of 50 monomer units); again, this implied

a dependence of the entry rate coefficient on surface coverage. The work of Adams et al. [3] refuted all these postulated mechanisms.

5.2. The 'control by aqueous-phase growth' ('Maxwell–Morrison') entry mechanism

The now accepted entry mechanism was developed by Maxwell et al. [62] in light of the extant experimental data on the radical entry process in emulsion systems, as well as further experimental work. Realizing that the data of Adams et al. [3] suggested that somehow the entry mechanism did not depend directly on any event occurring on the particle surface, the focus was shifted to the aqueous-phase propagation (and termination) prior to entry. The addition of a sufficient number (denoted z) of monomer units to an initiator-derived radical leads to a surface-active oligomer; the crucial step in the model is that the entry process of this z-mer is assumed to be so fast as to be diffusion-controlled (entry into a particle being its only possible fate). This allows the rate of entry to be equated to the rate of formation of z-mers, which can be easily achieved from the following chemical equations that govern the entry process:

$$\text{initiator} \xrightarrow{fk_d} 2\text{I}^\bullet \tag{36}$$

$$\text{I}^\bullet + \text{M} \xrightarrow{k_{pi}} \text{IM}^\bullet \tag{37}$$

$$\text{IM}^\bullet_{i-1} + \text{M} \xrightarrow{k_{pw}} \text{IM}^\bullet_i, \quad i < z \tag{38}$$

$$\text{IM}^\bullet_i + \text{T}^\bullet \xrightarrow{k_{tw}} \text{dead product}, \quad i < z \tag{39}$$

$$\text{IM}^\bullet_z + \text{particle} \xrightarrow{\rho_{init}} \text{entry} \tag{40}$$

where $\text{I}^\bullet$ is a radical derived from thermal decomposition of the initiator (dissociation rate coefficient k_d with efficiency f), M a monomer unit, $\text{T}^\bullet$ any aqueous-phase radical, $\text{IM}^\bullet_i$ an aqueous-phase oligomer containing i monomer units and $\text{IM}^\bullet_z$ a surface-active oligomer. The rate coefficients for propagation, termination and entry (all in the aqueous phase) are given by k_{pw}, k_{tw} and ρ_{init}, respectively. It is important to point out that Eq. (40) does not imply that every encounter between a 'z-mer' and a latex particle results in a true entry event (entry is normally considered to have been successful when the oligomer begins to propagate in the interior of a particle), as adsorption and desorption may occur numerous times; rather the only chemical fate that a z-mer undergoes will be entry.

Solution of the steady-state evolution equations corresponding to Eqs. (36)–(40) yields the following approximate analytic expression for ρ_{init}, namely:

$$\rho_{init} \approx \frac{2fk_d[\text{I}]N_A}{N_p}\left\{\frac{2\sqrt{fk_d[\text{I}]k_{tw}}}{k_{pw}C_w} + 1\right\}^{1-z} \tag{41}$$

The only unknown parameter within this model is the value of z; while the model is a simplification (as there will be oligomers that propagate beyond the length z), it helps to provide physical understanding to the kinetics as an 'average' degree of polymerization in the aqueous phase. It was shown [62] that excellent agreement with experimentally obtained entry rate coefficients for styrene/persulfate systems was obtained with a value $z = 2$–3 (Fig. 13).

To date, this model has provided agreement with all studies involving electrostatically stabilized latex systems [13,55,62,72,73] and is yet to be refuted. Indeed, experiments have been performed which had the potential to refute this postulate. Eq. (41) predicts that the entry rate coefficient should be independent of particle size, provided all other variables such as particle number and initiator concentration are kept constant. It is immediately apparent that no *ab initio* system could be used to carry out such a test, because any way in which particle size can be varied (e.g. by changing the concentration of surfactant or of initiator) will also change particle number. The design of a seeded experiment to carry out such a test is not straightforward, because of the need to avoid secondary nucleation while at the same time having two latexes with the same N_p but significantly different particle sizes. Nevertheless, when appropriate conditions were found, this simple implication of Maxwell–Morrison model, independent of ρ_{init} on particle size, was indeed observed experimentally [13].

The Maxwell–Morrison entry model also indicates that there should be no charge effect with regards to the charges on both the entering radical and the particle surface. van Berkel et al. [55] studied the effect of altering the sign of the charge on both the particle surface and the initiator for styrene emulsion polymerizations, and no change in the kinetics was seen – in agreement with the assumptions made within the entry model.

Maxwell–Morrison entry model predicts the contribution to the entry rate coefficient made from the added chemical initiator; the overall entry rate coefficient, however, ρ is actually

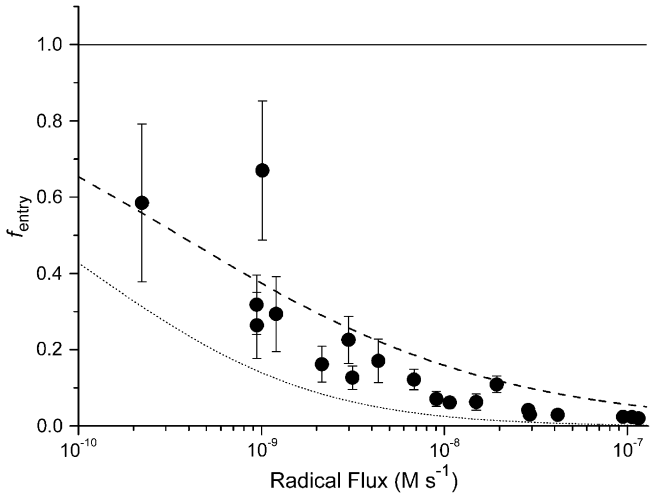

Fig. 13. Agreement between the 'control by aqueous-phase growth' entry mechanism and experimentally determined entry efficiencies (styrene/persulfate experiments) for $z = 2$ (broken line) and 3 (dotted line).

the sum of the initiator and 'spontaneous' entry rate coefficients. Many monomers, such as styrene and chlorobutadiene [54], undergo non-negligible amounts of emulsion polymerization in the absence of any added chemical initiator. The exact origin of this spontaneous polymerization is unclear – it is often thought that residual peroxides that are formed on the particle surface during seed latex synthesis may break down when the latex is polymerized further, leading to the generation of additional radical species. It has also been shown that, in the case of styrene, a Diels–Alder rearrangement reaction [74] can generate a radical that can initiate polymerization.

5.3. Thermodynamic rationalization

The concept of the critical degree of polymerization z in 'Maxwell–Morrison' model for radical entry can be understood from thermodynamic reasoning – it is essentially the number of units required to impart surface activity to the species in question. All radicals will encounter a latex particle at some time; however, the criterion of surface activity ensures that the radical is less likely to desorb and more likely to enter. The larger the equilibrium constant is in favour of adsorption (i.e. the greater the hydrophobic free energy $|\Delta G^{\mathrm{hyd}}|$), the more likely a true entry event will take place.

For a hydrophobic monomer such as styrene with low water solubility, the hydrophobic free energy of a monomeric unit is approximately given by:

$$\Delta G^{\mathrm{hyd}} \approx RT \ln C_{\mathrm{w}}^{\mathrm{sat}} \tag{42}$$

(where here and below the argument of the logarithmic term is the activity, a dimensionless quantity which for dilute solutions such as this is numerically equal to the concentration in M). For the case of styrene, ΔG^{hyd} is $-15\ \mathrm{kJ\ mol^{-1}}$. The degree of polymerization for surface activity depends on the ionic group. The sulfate ion radical is extremely hydrophilic, so one must determine how many styrene units would have to be added to such a radical to impart surface activity. Using aliphatic alkyl sulfates as model compounds [75], it was seen that $|\Delta G^{\mathrm{hyd}}| \approx 23\ \mathrm{kJ\ mol^{-1}}$ is the minimum value of the hydrophobic free energy to impart surface activity. It can be seen simply that for styrene in this case the addition of two styrene units will satisfy this criteria, i.e. $z = 2$. For persulfate-initiated systems, the value of z can thus be calculated from the following formula:

$$z = 1 + \mathrm{int}\left(\frac{-23\ \mathrm{kJ\ mol^{-1}}}{RT \ln C_{\mathrm{w}}^{\mathrm{sat}}}\right) \tag{43}$$

where the 'int' function rounds the quantity in the brackets to the lower integer value. This expression allows the value of z for other monomers with persulfate initiator to be determined; for example this predicts $z = 4–5$ for the more water-soluble methyl methacrylate (MMA) (i.e. a more water-soluble monomer will have to add more units in the aqueous phase before it becomes surface active). Direct experimental evidence for the value of z in MMA systems was seen in the work of Marestin et al. [76], who added a radical trap onto the surface of a poly(MMA) latex particle; the maximum degree of polymerization of the trapped oligomers was found to be 5, in agreement with Maxwell–Morrison mechanism.

Eq. (43) is only applicable for determining the value of z in persulfate-initiated systems; the relative hydrophilicity of the initiating radical is important, and changes the free-energy term from the persulfate/styrene value of 23 kJ mol^{-1}. In general, for the same monomer, the more hydrophilic the primary radical from initiator, the greater the value of z. van Berkel et al. [55] demonstrated that for the positively charged initiator V-50 (2,2′-azobis(2-amidinopropane)), $z = 1$ for styrene, while Thickett and Gilbert [61] showed that for the neutral azo initiator VA-086 (2,2′-azobis[2-methyl-*N*-(2-hydroxyethyl)propionamide]) $z = 3$ (this larger value of z is simply due to the fact that the primary radical formed from this initiator is extremely water-soluble). The hydrophobic free energy needed to overcome the water solubility of the initiating fragment can potentially be estimated from functional group contribution tables [77] for any initiator.

The rate coefficient ρ_{init} is, as has been mentioned, a pseudo-first-order rate coefficient – in the case of Maxwell–Morrison model it can also be written as $k_{\mathrm{e}}[\mathrm{IM}_z^{\bullet}]$, where k_{e} is the second-order rate coefficient for radical entry, and $[\mathrm{IM}_z^{\bullet}]$ the concentration of z-mers in the aqueous phase. Smoluchowski equation for diffusion-controlled reactions can be used to estimate k_{e}, namely:

$$k_{\mathrm{e}} = 4\pi D r_{\mathrm{s}} N_{\mathrm{A}} \tag{44}$$

where D is the diffusion coefficient of the entering species in the aqueous phase. It can be seen that k_{e} is predicted to be a linear function of r_{s}. In the case of a bimodal particle size distribution (PSD), the relative rates of capture will be related to the size of the particles in question – entry will most likely occur into the larger of the two particles. Experiments performed by Morrison et al. [78] where a bimodal poly(styrene) emulsion was polymerized (known as 'competitive growth' experiments) demonstrated that the ratio of entry rate coefficients of the two sets of particles was equal to the ratio of the radii, in accordance with that predicted by the entry model. It should be pointed out, however, that these were very specific experiments; in the much more typical case of the polymerization of a monomodal PSD the pseudo-first-order entry rate coefficient ρ is independent of particle size (assuming all other parameters are kept constant).

Strong support for the fundamental hypothesis that the entry rate of a z-mer is so fast as not to be rate determining comes from recent work by Hernandez and Tauer [79] using Monte Carlo simulations, who showed that the capture rate of a small species at higher volume fractions of particles is significantly greater (up to a factor of 10 at the highest volume fractions) than Smoluchowski rate. This strengthens the arguments as to the fate of exited radicals illustrated in Fig. 8.

5.4. Recent investigations of entry

Radical entry has remained an often studied event since the development of the 'control by aqueous-phase growth' mechanism and the associated supporting experimental evidence. Asua and De la Cal [80] carried out extensive modelling of styrene emulsion polymerizations to determine the behaviour of the rate coefficients of entry and exit as a function of particle size. Their results demonstrated that the rate coefficient of entry was essentially independent of particle size, in line with a propagational mechanism governing the process (as opposed to diffusional, collisional or colloidal).

Kim and Lee [81] considered one of the key assumptions of Maxwell–Morrison mechanism that upon reaching the critical length z, the radical is instantaneously and irreversibly captured by a particle regardless of what occurs in the particle interior. By stating that the rate of radical entry is a function of what occurs in the particle interior (be it propagation or termination), the rate of entry is related to the flux at the particle surface and a 'transient' entry rate can be calculated. It was shown through this modelling that besides the first few seconds of the overall reaction, the magnitude of the steady-state entry rate is unchanged and the assumptions of Maxwell–Morrison approach are in general robust and correct.

Radical entry involving other monomers has also been studied. Kshirsagar and Poehlein [82] studied radical entry in seeded emulsion polymerization experiments involving vinyl acetate with a poly(styrene) seed. The seed latex was doped with a water-insoluble inhibitor to capture and form stable oligomers of poly(vinyl acetate), in order to determine the critical DP for entry in this system. Fast atom-bombardment mass spectrometry was used to determine the size of the formed oligomers; results showed that the critical length for entry in this system was 5–6 monomer units, in line with the predicted value from Maxwell–Morrison entry mechanism on thermodynamic grounds. De Bruyn et al. studied the kinetics of vinyl neodecanoate [73], an extremely water-insoluble monomer. The combination of chemically initiated and γ-initiated seeded dilatometry experiments provided experimental data in support of the developed entry mechanism; due to the extremely low monomer solubility in water, the critical length z was only 1–2 units in this case.

Dong and Sundberg [83] developed a lattice model to estimate the change in free energy of oligomers of differing lengths as adsorption onto a latex interface took place. The variation of this free-energy term allowed for estimation of the critical length z where entry (and adsorption) is spontaneous; theoretically derived values of z were in excellent agreement with experiment. The developed model also allowed for estimating critical lengths for entry in co-monomer systems, revealing that the sequence distribution within the oligomer itself had little effect on the value of z. Further modelling [84] took into account the propagation step at the water/latex interface in the overall entry mechanism; this is of particular importance in monomer-starved experimental conditions where propagation may be rate determining. Results again supported Maxwell–Morrison assumptions.

The concept of propagation to a critical length z has recently been challenged by the group of Tauer [85], who claimed that primary initiator-derived radicals (such as the sulfate ion radical) can directly enter latex particles without addition of any monomer units. This was claimed on the basis of experiments where latexes containing RAFT agents had the RAFT agent destroyed/modified by the introduction of potassium persulfate into the system, in the absence of any monomer. The work of Goicoechea et al. [86], however, proved that this result was most likely due to the complicated decomposition mechanism of persulfate ions that can regularly lead to the generation of the more hydrophobic hydroxyl radical. Experiments where hydroxyl radical generation was suppressed demonstrated that this effect was no longer observed. While persulfate-initiated emulsion polymerization experiments can lead to the formation of radicals that can directly enter latex particles, this most likely represents a small contribution to the overall entry process that is governed by aqueous-phase propagation.

5.5. Entry in electrosterically stabilized systems

The rate coefficient for radical entry in electrosterically stabilized systems has only been studied recently. For 'uncontrolled' latexes (i.e. the electrosteric layer had been synthesized using conventional free-radical polymerization, affording no molecular weight control or control of the architecture of the hairy layer), it was seen that ρ was reduced relative to that predicted by Maxwell–Morrison entry mechanism. This reduction was seen to be a function of the surface coverage of the latex by poly(acrylic acid), as well as varying with the pH of the emulsion. The biggest problem in this work was that extensive secondary nucleation took place at high particle numbers [58], rendering the extraction of rate coefficients ambiguous at best. Nonetheless, a significant reduction in rate was seen.

The same result was seen using latexes made under molecular weight control by the RAFT method [61] – the experimentally determined entry rate coefficients were, in this case, more than an order of magnitude lower than that predicted by the expected entry mechanism. The steady-state ρ values in this work, however, were calculated assuming Limit 2a kinetics, i.e. a monomeric radical desorbs into the aqueous phase, where it will re-enter another particle (Eq. (35), Limit 2a). However, the Limit 1 expression (which only has a linear dependence on $\overline{n}_{ss}$ rather than a quadratic dependence, a significant effect when dealing with very low values of $\overline{n}_{ss}$ as seen in this work), yields good agreement with Maxwell–Morrison model for styrene with three different types of initiators with different z values, suggesting termination rather than re-entry as the dominant loss fate. This unexpected result was the catalyst for the development of an extended kinetic model [65]. Formation of mid-chain radicals in acrylate systems is a well established phenomenon [87–90]. The new treatment considered a variety of radical-loss fates occurring simultaneously – standard radical desorption, transfer to a poly(AA) site and termination with a mid-chain radical

in the hairy layer, where it was shown that transfer/termination before exit was dominant. This is the standard Maxwell–Morrison mechanism together with a new step, the formation of radicals in the hairy layer which are slow to propagate but quick to terminate. This immediately rationalized the first-order loss mechanism which, when applied to experimental data, gave agreement with Maxwell–Morrison model.

The extended model implies that the entry event (a diffusion-controlled process, Eq. (44)) is still orders of magnitude more likely than a transfer/termination event on the particle surface (the reverse is not true for exit, where the rate of desorption is less than transfer/termination for small particles). Only for extremely small particles would the entry process be affected in any way in these systems.

By considering the various radical-loss fates in these systems, the newly developed kinetic model was able to predict accurately the results obtained in 'uncontrolled' systems such as those studied by Vorwerg and Gilbert [58]; modelling the behaviour of these electrosterically stabilized systems with an accuracy never before is achievable.

6. Radical termination

6.1. Termination reactions

Bimolecular radical termination, leading to the loss of two growing polymer chains, is by far the most complicated of the fundamental reactions that govern any type of polymerization, be it bulk, solution, emulsion or any other process [18,91]. Growing radicals can terminate via one of the two processes – combination and disproportionation. While the mode of termination is one of the determining events in the molecular weight distribution of the evolved polymer, from the kinetic perspective of the present review it is only important that it is a reaction that leads to loss of radical activity.

Termination in a condensed phase can be said to involve three steps [92]: (1) chain encounter, i.e. the two chains bearing radical end groups must diffuse into within reasonable proximity of each other, a process governed by centre-of-mass diffusion; (2) the radical chain ends must encounter each other, a process governed by segmental diffusion of the units of the polymer chain; (3) the final step, the actual termination reaction, is relatively quick on the timescale of these diffusion-controlled events: for example, the activation energy of recombination is essentially zero [93], and this third step is not rate determining in the condensed phase. The dominant events in termination at low polymer concentration are still a matter of debate [18,91,94].

Happily, the situation in an emulsion polymerization is actually simplified. This is because the polymer concentration in a particle is always above c^{**}, that for entanglement between chains. This is readily seen from values of the equilibrium monomer concentration within particles, C_p^{sat}, which are typically ~4 to 6 M, and correspond to a weight-fraction polymer concentration $w_p \sim 0.3–0.4$, much greater than typical values of c^{**}. This has the overall result that the dominant event in termination in emulsion polymerizations is expected to be the diffusion of a relatively small (and hence mobile) radical resulting from initiator or from transfer with a much longer (and hence relatively immobile) radical chain. This is illustrated in Fig. 14, which shows the rate of termination $k_t^{ij}R_iR_j$ of Eq. (21) as a function of the degrees of polymerization of the two radicals, calculated using the diffusion model described below. It is readily seen from this plot that indeed the termination rate is greatest when one of the chains is small (note the axes are all on a logarithmic scale).

As monomer is converted to polymer, the bulk viscosity increases, and hence the diffusion coefficient of a short radical decreases with conversion, and hence so does the termination rate. Indeed, direct measurements (e.g. [95]) show that $\langle k_t \rangle$ can vary by several orders of magnitude during the one reaction. This is an important consideration from a data processing perspective, as k_t values determined from bulk experiments at very low conversion could not be used to process data from an Interval II (or III) emulsion polymerization experiment, where the weight fraction of polymer (w_p) within the particles is considerably higher.

The most important consideration regarding the termination process is that the termination rate coefficients are chain-length dependent. The diffusion of polymeric chains decreases significantly as the degree of polymerization increases [96], meaning that the termination rate coefficient measured from experimental data will only be an average ($\langle k_t \rangle$) across all chain lengths considered. Significant work has been done in understanding and modelling the nature of chain-length-dependent termination. Unfortunately there are as yet no direct measurements of individual values of k_t^{ij} in conventional free-radical polymerizations at conversions of importance in emulsion polymerizations. On the other hand, there has been considerable advances (e.g. [97–99]) in obtaining data for

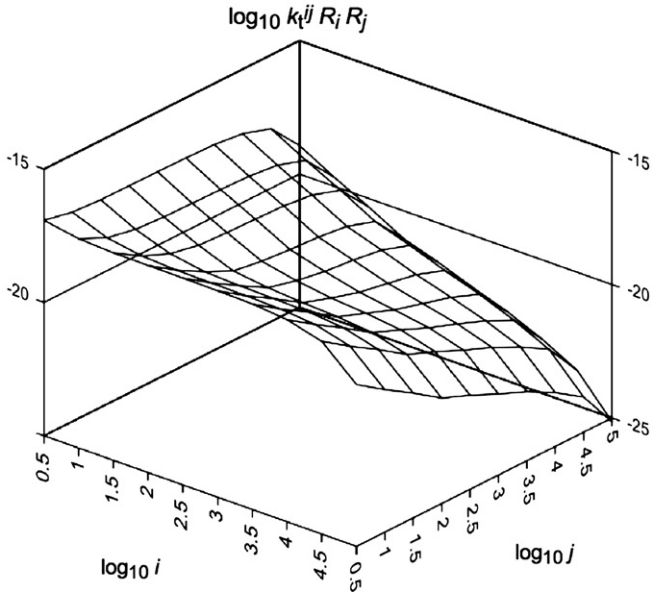

Fig. 14. Termination rate ($M\,s^{-1}$) for the termination between individual chains of degrees of polymerization i and j, using the diffusion model in the text. Note all axes are logarithmic.

k_t^{ii}, i.e. when both chains are of the same degree of polymerization, which is of importance in *controlled*-radical polymerization in emulsion.

The best model to use to calculate the termination rate coefficient at values of w_p of importance for emulsion polymerizations is that of Russell and others [15,19,31,94,100–104], which is now summarized. It is based on the assumption that termination is diffusion-controlled, and that the diffusion coefficient of a chain of degree of polymerization i can be determined from that of a monomeric chain at the same w_p through an empirical scaling "law" fitted to a range of data on diffusion of oligomers up to degree of polymerization 10 in a wide range of monomer/polymer mixtures [105–107]. The chain-length-dependent termination rate coefficient is taken to be given by:

$$k_t^{ij} = 2\pi p\left(D_i + D_j\right)\sigma N_A \tag{45}$$

Here D_i and D_j are the diffusion coefficients of the radical ends of an i-mer and a j-mer, p is the probability of reaction upon encounter, which may be less than one because of the effects of spin multiplicity [104], and σ is the Lennard-Jones diameter of a monomer unit. The quantity p takes account of the radicals being in doublet spin states, and the probability is 1/4 that two free radicals will have opposite spin and so be able to combine (which requires that they be on the singly-degenerate singlet surface rather than the triply-degenerate triplet one). Thus at low conversion, one expects $p = 1/4$. However, in the condensed phase, especially as the system goes through the glass transition, two adjacent free-radical ends may be trapped within a solvent cage sufficiently long enough to allow the spins to flip, when one would have $p = 1$. In a glassy polymeric system, it is reasonable to put $p = 1$. Because p always appears as the product pD_{mon} (where D_{mon} is the diffusion coefficient of a monomer radical – see below), these two quantities comprise a single unknown parameter whose value can be estimated from independent information [104].

There are two components to each D_i: centre-of-mass diffusion, with diffusion coefficient D_i^{com}, and diffusion by propagational growth of the chain end ('reaction-diffusion'), with diffusion coefficient D^{rd}. Hence:

$$D_i = D_i^{com} + D^{rd} \tag{46}$$

The rigid-chain-limit model [108] is used for D^{rd}:

$$D^{rd} = \frac{1}{6} k_p C_p a^2 \tag{47}$$

where a is the root-mean-square end-to-end distance per square root of the number of monomer units in a polymer chain. The value of a was taken as suggested from earlier studies [109]. To specify the chain-length variation of the self-diffusion coefficient D_i^{com} for the diffusion coefficient of polar monomer in monomer/polymer solution, a scaling law was assumed:

$$\frac{D_i(w_p)}{D_{mon}(w_p)} \approx i^{-u} \tag{48}$$

with the empirical relation [105–107]:

$$u = 0.66 + 2.02 w_p \tag{49}$$

modified to take into account the 'composite' model of Russell and co-workers [32,110].

The k_t^{ij} obtained with this model is then used to solve Eq. (21) in the steady state using numerical methods developed by Clay and Gilbert [19] (which require trivial computational resources to evaluate), thereby yielding $\langle c \rangle$. The results of these calculations have only thus far been compared to limited experimental data for emulsion polymerizations: for styrene [111] and MMA [15]. The accord is acceptable, given the uncertainties in the various rate parameters such as the diffusion coefficients (and their scaling with degree of polymerization) and transfer constants. While this accord is not of sufficient accuracy for precise prediction, it is such that it supports the basic premises of the model.

Smith and Russell [112] have pointed out that termination rates can be categorized as being either 'transfer' or 'termination' limited. Both styrene and MMA fall into the transfer-limited category. This category is where most termination is when one of the chains is an oligomer resulting from transfer to monomer. It must be emphasized that this does not imply that the termination rate coefficient is simply that of transfer; Russell has given an extensive discussion of this point.

An example of comparison between $\langle k_t \rangle$ values obtained from experiment using γ radiolysis [111,113] and the model is shown for styrene in Fig. 15. The dependence on D_{mon} on w_p used was taken from pulsed-field-gradient NMR measurements [107]. In this comparison, minor changes (up to a factor of 2) were made in the various rate parameters stated above to have some uncertainty.

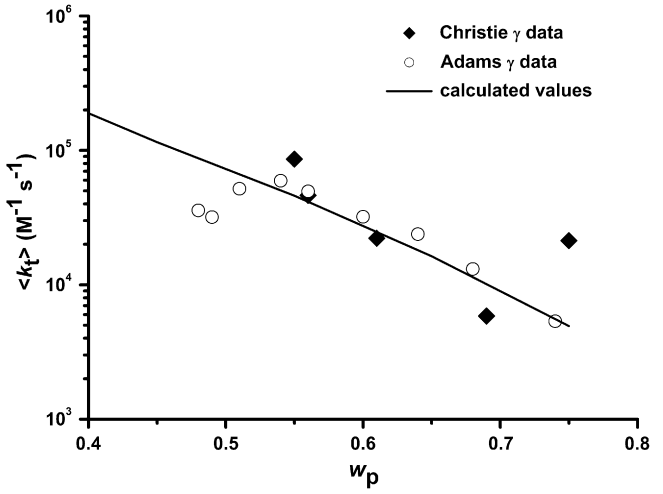

Fig. 15. Average termination rate coefficient: in styrene emulsion polymerization: comparing data obtained from γ radiolysis [111,113] and those from the model (wherein minor adjustments to parameters were made). The data are for large particles, whose kinetics are in the pseudo-bulk limit and this radical loss is dominated by termination.

7. Particle formation

7.1. The fundamentals of particle formation

A detailed understanding of the mechanisms that govern particle formation is crucial for a complete understanding of emulsion polymerization; for example, this governs the final particle size/number in an *ab initio* system. Similarly, understanding the conditions that avoid the formation of new particles in seeded systems (secondary nucleation) is vital for a number of industrial procedures (for example, a crop of new particles can ruin surface-coating properties of a paint). Particle formation mechanisms are complex, and the understanding developed through particle growth (namely radical entry and exit, and aqueous-phase events) is critical to understand the formation mechanism.

Particle formation has been a long-studied area of emulsion polymerization research, and due to an incomplete mechanistic picture, false conclusions can often be reached. As an example, Smith and Ewart's [14] pioneering work in the consideration of micellar nucleation suggested that the final particle number is proportional to $[I]^{0.4}[S]^{0.6}$ where [I] and [S] are the concentrations of initiator and surfactant, respectively. Much subsequent work that demonstrated such a dependence was cited as proof of the micellar nucleation mechanism in operation; however, Roe [114] showed that the same exponents can be predicted from a homogeneous nucleation model. Fitch [115] and Gardon [116,117] also experimentally demonstrated a wider range of exponents. Indeed, a typical experimental dependence of particle number on [S] is sigmoidal in shape, so that a region can be found to agree with most exponents, and such selectivity was all too common in the early literature.

One aim of understanding particle formation is to be able to predict and explain the dependence of N_p on the surfactant concentration, initiator concentration, temperature and the monomer(s) used. N_p depends strongly on [S], but a limiting value exists as [S] approaches zero. The most rapid variation of N_p with [S] occurs near the critical micelle concentration (CMC). It is generally accepted that there are two principle nucleation processes in particle formation: *micellar nucleation,* which predominates above the CMC, and *homogeneous nucleation*, which predominates below the CMC. A third mechanism, *droplet nucleation*, which historically was the original basis for trying to create an emulsion polymerization, in fact only occurs very rarely; those cases are (1) in some systems such as chlorobutadiene which have a very large spontaneous initiation component [54], (2) the special systems [118] of miniemulsion polymerization and microemulsion polymerization (which are not considered in the present review), and (unintentionally) in controlled-radical systems which fail to take this into account in their design [40,119].

It was shown in Section 5 that the growth of initiator-derived radicals in the aqueous phase comprises one of the key steps of 'Maxwell–Morrison' entry mechanism [62]. This mechanism can be generalized to *ab initio* systems: the three mutually exclusive fates for a radical (besides propagation) become terminated, entry into a pre-existing particle and *creation of a new particle*. Interval I in an *ab initio* system involves the formation of particles through an appropriate mechanism; new particles can be formed in a seeded experiment as well in what is known as secondary nucleation.

Particle formation cannot instantaneously start or stop – it occurs over a finite time period. It is, however, important to know when particle formation predominantly begins or ends. Whichever particle formation mechanism is dominant, the process will stop when enough particles have been generated to capture the entire population of surface-active (z-meric) radical species. For example as the particle number increases in an emulsion polymerization (and they increase in size as the polymerization takes place), the likelihood of capturing a z-mer becomes so high as to make new particle formation essentially impossible. Numerical quantification of these fates and the modelling of relevant mechanisms are crucial in elucidating the appropriate mechanism in emulsion polymerization systems.

7.2. Experimental methods of investigating particle formation

Many experimental techniques are available to study particle formation, although despite decades of effort and the investment of considerable resources by industry and academia using techniques such as stop-flow, it has proved impossible thus far to observe particle nucleation directly. All data obtained thus far on nucleation are more or less indirect. A key criterion to the success of any technique is the ease of measurement of the desired quantity without perturbing the system (through for example, the introduction of oxygen into the reaction medium when taking samples at different time periods) and treating data with a minimal number of model-based assumptions. Some techniques are listed below.

7.2.1. Rate data

Eq. (25) relates the rate of change of fractional conversion to $\overline{n}$, N_p and a variety of other constants. Normally this equation is used for seeded experiments that commence in Interval II or III; for the purpose of studying particle formation, rate data for Interval I must be obtained. The biggest difficulty in processing Interval I data is that at early time periods in an *ab initio* experiment, newly formed particles are very small and the monomer concentration inside the particles, C_p, is not constant. This is due to the variation of the surface free energy of the particles as a function of size, as seen in Morton equation [9]. However, Morton equation cannot be trusted to accurately predict C_p as a function of the particle radius (as Flory–Huggins interaction parameter χ and the interfacial tension between latex particles Γ needed to solve Morton equation can only be obtained through measurement of C_p, and moreover the value of χ so obtained is different from that from bulk measurements, indicating the quantitative unreliability of the theory [120]). Thus use of rate data from Interval I to model nucleation mechanisms is difficult at best.

7.2.2. Surface tension and viscosity measurements

Changes in surface tension during an emulsion polymerization have long been used to monitor nucleation. In the case of

an *ab initio* emulsion polymerization under 'starved-feed' conditions, the start of the experiment is simply the aqueous-phase polymerization of the monomer in question. As a result, the formation of surface-active oligomers can be determined by monitoring the surface tension as a function of time; this occurs when the surface tension drops sharply as these molecules begin to aggregate. This provides a means to determine the time of onset of particle formation, as well as the degree of polymerization at which growing chains become surface active. As shown by Hergeth et al. [121,122], the surface tension increases after this initial decrease, with the rapidity of this increase to a constant value related to the duration of particle formation and to how much generated surface area is required to capture subsequently formed oligomers. Similar results can be obtained through the monitoring of the specific viscosity in starved-feed systems. Again, the onset of particle formation is marked by a sudden drop in the specific viscosity; however, a local maximum in this value is seen as a function of conversion, perhaps due to aggregation of these precursor particles ('homogeneous-coagulative nucleation' [123–125]) and the inclusion of water within this aggregate. True coagulation and formation of a mature latex particle lead to the densification of these aggregates and another subsequent decrease in the specific viscosity [122].

7.2.3. Molecular weight distribution data

As particle formation in *ab initio* systems is usually finished in the first 5–10% of the total time period over which polymerization takes place, only molecular weight distributions from samples taken very early would reveal important mechanistic information regarding particle formation. Often this involves taking samples from the reaction vessel at regular time intervals early in the polymerization process – great care must be taken not to introduce oxygen into the reaction during this process, as oxygen acts as a polymerization inhibitor.

7.2.4. Particle size and number

N_p is governed by the particle formation mechanism taking place in the system being studied, and (unless secondary nucleation occurs) the value of N_p remains constant until the end of the reaction, well after the end of the nucleation period has ended. As a result, examining the behaviour of N_p as a function of initiator and surfactant concentrations is an ideal means to test nucleation mechanisms. N_p is simply determined from particle size measurements (Eq. (1)) which also allow the determination of any secondary nucleation through a crop of new particles in seeded experiments. While this is in essence examining particle formation 'after the event,' the reliability in accurate particle size and N_p measurements allow for a significant amount of mechanistic information to be obtained from such experiments.

7.2.5. Particle size distribution measurements

Information regarding particle formation mechanisms can be obtained from the particle size distribution (PSD) during Interval I; however, interpretation is again difficult due to the inability to predict C_p as a function of particle size with any degree of precision, and also the inaccuracy of all extant means of determining PSDs with high accuracy where very small and polydisperse particles are present. It is noted that PSD data have been used to refute by the author's laboratory to refute one of our own mechanistic postulates, viz., that micelles may not be involved above the CMC [126].

7.2.6. Calorimetry

On-line monitoring of calorimetry can prove to be a useful tool to determine the onset of particle formation. In the case of an *ab initio* experiment, the heat flow from the reaction shows a sharp increase at the onset of nucleation; this is because particles provide a monomer-rich site for rapid polymerization (an exothermic process). The time between the increase in heat flow and reaching a constant flow represents the timescale for the entirety of Interval I. This technique has proven successful in understanding particle formation in controlled-radical polymerization systems [127,128], where amphiphilic diblock copolymers self-assemble in the aqueous phase to form latex particles under starved-feed conditions where the particle formation time is long.

7.3. Particle formation in electrostatically stabilized systems: below the CMC

Micelles can play an important role in the nucleation process. Particle formation below the CMC means that the complication of micelles in the aqueous phase need not be considered.

The dominant particle formation mechanism under these conditions, *homogeneous nucleation* [129], is illustrated in Fig. 16. An initiator-derived radical propagates with the small amounts of monomer in the aqueous phase (mechanistically identical to the construction of the 'control by aqueous-phase growth' entry mechanism), but propagation continues beyond the length z (where surface activity is attained) to a length j_{crit} – the critical chain length before the growing oligomer is no longer soluble in the aqueous phase, or to be more

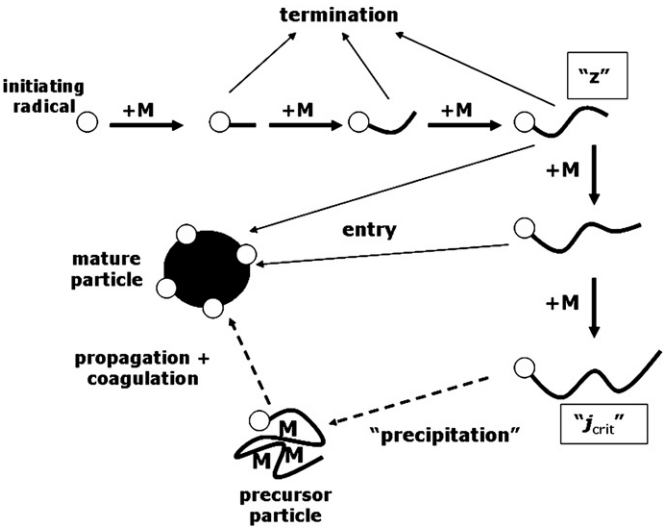

Fig. 16. Representation of the homogeneous nucleation mechanism.

precise undergoes a coil-to-globule transition. This transition excludes water, forming a precursor particle that can become swollen with monomer; these precursor particles either grow via propagation or coagulation with other precursor particles to form a stable particle. This model was first put forward by Fitch and Tsai [130], with the mathematical quantification of this mechanism known as the 'HUFT' (Hansen, Ugelstad, Fitch and Tsai) model [16]. The value of j_{crit} was estimated on thermodynamic grounds in the work of Maxwell et al. [62] by considering Krafft temperature for a series of *n*-alkyl sulfates; for example, it was shown that for styrene that a pentameric radical should be water-insoluble, i.e. $j_{crit} = 5$. This value was consistent with the work of Goodall et al. [131], who analyzed the molecular weight distribution of the water-insoluble component of surfactant-free emulsion polymerization experiments and saw that the lowest molecular weight observed corresponded to a degree of polymerization of 10, i.e. the termination product of two pentamers.

Quantification of the HUFT model for homogeneous nucleation is an extension of the aqueous-phase kinetics considered for the radical entry mechanism (Eqs. (36)–(40)); that is, propagation beyond the length z is now permitted (with entry occurring at all lengths greater than z in the case of seed particles being present), as well as radical termination of all chain lengths. A new particle is deemed to have formed when a radical attains the degree of polymerization j_{crit} (naturally this is a simplification as a precipitated single chain will be highly unstable and prone to coagulation, but this model serves as an excellent starting point). These extra terms can be written as:

$$IM_i^{\bullet} + M \xrightarrow{k_{pw}} IM_{i+1}^{\bullet}, \quad i \geq z \tag{50}$$

$$IM_i^{\bullet} + T^{\bullet} \xrightarrow{k_{tw}} \text{dead product}, \quad i \geq z \tag{51}$$

$$IM_i^{\bullet} + \text{old particle} \xrightarrow{\rho_{init}} \text{entry}, \quad i \geq z \tag{52}$$

The resultant evolution equation for these extra terms is given by:

$$\frac{d[IM_i^{\bullet}]}{dt} = k_p C_w([IM_{i-1}^{\bullet}] - [IM_i^{\bullet}]) - k_{tw}[IM_i^{\bullet}][T^{\bullet}] - k_e^i[IM_i^{\bullet}]\frac{N_p}{N_A}, \quad z \leq i \leq (j_{crit}-1) \tag{53}$$

and the rate of particle formation is given by:

$$\frac{dN_p/N_A}{dt} = k_{pw} C_w [IM_{j_{crit}-1}^{\bullet}] \tag{54}$$

The evolution equations for these processes are easily solved numerically in the steady state, allowing determination of the rate of particle formation in these systems. The k_e^i in Eq. (53) represents the process of entry if an *i*-mer ($i \geq z$) given by the diffusion-controlled Smoluchowski equation (Eq. (44)), with the diffusion coefficient being D_i (the diffusion coefficient of an *i*-meric radical in water) and critical radius being r_s. This gives a time-dependent expression for k_e^i [2] that allows one to perform model calculations to calculate N_p as a function of reaction conditions. Typical parameters used in the case of styrene are presented in Table 2.

Table 2
Parameters for modelling particle formation in styrene emulsion polymerization experiments

Parameter	Value (styrene, 323 K)
z	2
j_{crit}	5
k_p	260 $M^{-1} s^{-1}$
k_p^1	$4k_p$
C_w	4.3×10^{-3} M
C_p	6 M
k_d (KPS)	1×10^{-6} s^{-1}
D_w	1.3×10^{-9} $m^2 s^{-1}$
k_t	1.75×10^9 $M^{-1} s^{-1}$

It can be seen (Fig. 17) that the calculated particle number shows a rapid increase in the first few seconds of the reaction, almost reaching its steady-state value. The rate of formation of new particles, however, decreases very quickly as the rate of radical entry becomes significant; as $z < j_{crit}$, the likelihood of radical capture by a formed particle is much greater than forming a new particle. The use of this extended HUFT model to predict the final particle number as a function of temperature for monomers such as styrene and MMA [132] for zero-surfactant systems proved to be in semi-quantitative agreement with experiment; however, the model poorly replicates data where the particle number is studied as a function of the initiator concentration [I]. Model predictions suggest a decrease in N_p as [I] is increased, as termination (a second-order process) at high radical fluxes suppresses particle formation – however, the reverse is seen experimentally when the ionic strength is held constant [132]. Similarly a decrease in N_p is observed as the total ionic strength is increased, something not predicted by the homogeneous nucleation model. This failure is attributed to no allowance for the coagulation of precursor particles to form a stable moiety in this treatment, an extension that considers the kinetics of these precursor particles as a function of their volume. Inclusion of coagulation

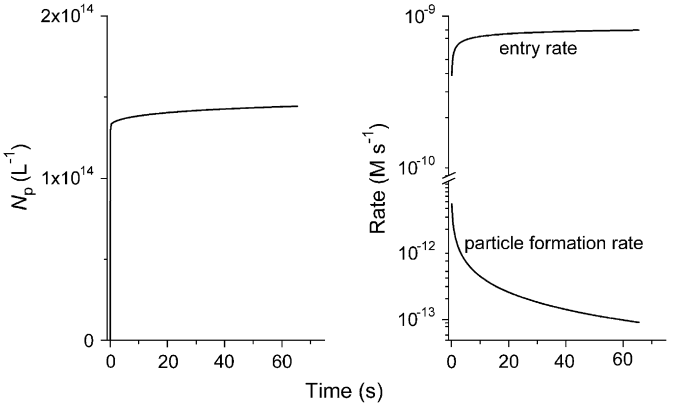

Fig. 17. Calculated variation of N_p as a function of time for the homogeneous nucleation mechanism (left panel); Variation of the rates of particle formation and radical entry as a function of time (right panel).

terms into the appropriate evolution equations is known as the 'homogeneous-coagulative' treatment [123,124].

Rapid hetero-coagulation (coagulation between precursor particles of different sizes, possible due to the rearrangement of electrical double layers of differing curvatures) has been quantified [133,134]; however, to model this requires knowledge of the form of the coagulation rate coefficient between small particles of different sizes, for which there is no experimental information. An extended version of the DLVO model can be used to represent these terms, the details of which are given elsewhere [124]. The inclusion of these coagulation terms does allow for semi-quantitative agreement with experiment in the case of variation of ionic strength; however, a number of model-based assumptions and adjustable parameters are introduced as a result. For many purposes the simple homogeneous nucleation model is adequate.

This homogeneous nucleation model has proven successful for the quantification of the amount of secondary nucleation in systems below the CMC [135–138]. Eq. (53) can be extended to allow for two populations of particles to be present – the seed particles N_{seed} and the newly formed particles N_{new}. Numerical solutions are again rapidly obtained for these systems, and comparison with experiment is possible through counting the ratio of new to old particles (for example, from a transmission electron microscopic (TEM) image or from a separation technique). It can be seen that the homogeneous nucleation model predicts that the amount of secondary nucleation for a seed latex of given size, beyond a seed particle number of $N_p \approx 10^{14}\,L^{-1}$ secondary nucleation is essentially insignificant (see Fig. 18) and need not be considered in the overall kinetics of the system; this, however, is sensitive to the particle size (and hence capture efficiency) of the seed latex in question. While more sophisticated nucleation models can be used which include the above treatment as a special case, this simple treatment provides an excellent insight into the conditions that ensure secondary nucleation is 'switched off.'

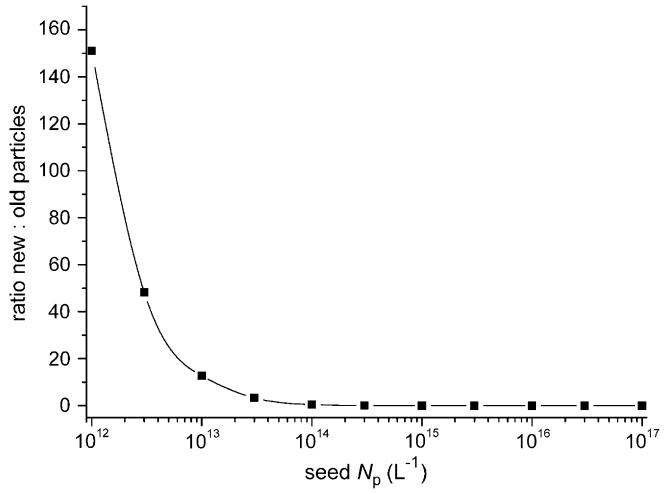

Fig. 18. Predicted amounts of secondary nucleation in styrene emulsion polymerization systems (323 K) as a function of seed particle number (seed latex diameter 146 nm), [persulfate] = 1 mM.

7.4. Particle formation in electrostatically stabilized systems: above the CMC

Particle formation above the CMC takes place in the presence of micelles. The original Smith–Ewart model [14], of which the foundations of the 'micellar nucleation' mechanism that govern these systems is based, has been extended to account for the various phenomena which came to light after (and often as a result of) their pioneering work.

Smith–Ewart model assumes that the end of the nucleation period is when micelles are no longer present within the reaction medium. This occurs as particles grow, adsorbing more and more surfactant onto their surface – a critical surface area A_p must be reached for this to take place. The surface area of a single particle A_s at time t (that was formed at time t') is given by:

$$A_s(t,t') = \left[(4\pi)^{1/2} 3K(t-t')\right]^{2/3} \tag{55}$$

Here $K(t-t')$ is the rate of volume of growth per particle, given by:

$$K = \frac{k_p M_0 C_p}{N_A d_p} \tag{56}$$

where M_0 is the molecular weight of monomer. Assuming that nucleation ceases at a time when the total surface area of all particles is equivalent to the total area of surfactant molecules (given by $a_s[S]$ where a_s is the surface area occupied by a single surfactant molecules), gives the well known result that the final particle number is given by:

$$N_p = 5^{3/5}\frac{1}{3\pi^{1/5}}\left(\frac{k_d[I]}{K}\right)^{2/5}(a_s[S])^{3/5} = 0.696\left(\frac{k_d[I]}{K}\right)^{2/5}(a_s[S])^{3/5} \tag{57}$$

The simple Smith–Ewart treatment also assumes that $N_p \to 0$ as $[S] \to 0$, which is incorrect when considering experiments below the CMC; this requires addition of the homogeneous nucleation mechanism. The effects of compartmentalization (as seen to be important in the consideration of 'zero-one' systems discussed earlier) are also neglected in this model, yet are likely to be significant in small, newly nucleated particles.

An extension [2] of Smith–Ewart treatment, incorporating aqueous-phase chemistry of initiator-derived oligomers and homogeneous nucleation, is presented to account for the mechanism of particle formation above the CMC, and is sketched in Fig. 19. The key features are:

- The accepted 'control by aqueous-phase growth' mechanism [62] that assumes propagation and termination in the water phase until a critical length z, whereby the radical becomes surface active.
- Entry of a z-mer into a micelle, forming a precursor particle that begins to grow.

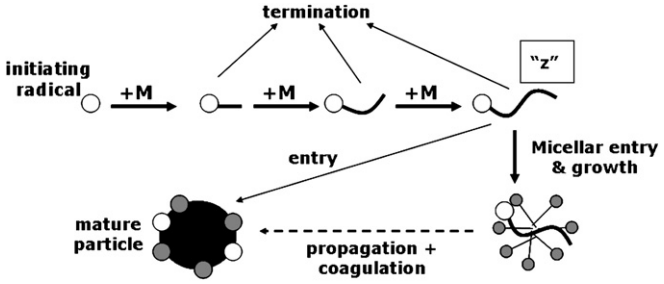

Fig. 19. Description of particle formation above the critical micelle concentration (CMC) of the surfactant used.

- Adsorption of surfactant onto the surface of these newly formed particles that gradually decrease the amount of free surfactant in the aqueous phase.
- Propagation in the aqueous phase beyond the length z to the length j_{crit} whereby the radical homogeneously nucleates a new (precursor) particle.
- Entry into and exit from precursor particles, while allowing for the possibility that a desorbed (monomeric) radical may be able to nucleate a new particle.

Once again, particle formation ceases when enough precursor particles have been established to capture the entire flux of aqueous-phase free radicals. It is noted that while micellar entry dominates above the CMC, homogeneous nucleation can still occur [139] (which, along with some 'local' micellar nucleation occurring just below the CMC, explains the well known observation [140] that when particle number is studied as a function of surfactant concentration, there is a more or less rapid, but not extremely steep, increase near the CMC). A comprehensive treatment that includes coagulation of precursor particles and compartmentalization effects, and intra-particle termination being rate determining, has been given [136,141], although a large number of unknown parameters are also introduced as a result. It is noted that while it is possible that z-mers might themselves form micelles [131,142–144], it has been shown [135] that this *in situ* micellization nucleation mechanism is unlikely to be a significant contributor to particle formation.

Of primary importance is to consider the entry event of a z-mer into a micelle. This can be done assuming that the entry event (as is the case with all entering radicals) is diffusion-controlled, and can be described by Smoluchowski equation:

$$k^i_{e,micelle} = 4\pi D_i r_{micelle} N_A, \quad i \geq z \tag{58}$$

where $r_{micelle}$ is the radius of a micelle. The various evolution equations for initiator-derived oligomers in the aqueous phase have exactly the same form as Eq. (53), except that an entry term into the micelle must be included for oligomers of length $\geq z$. The overall rate of particle formation, including the homogeneous nucleation contribution, is therefore:

$$\frac{dN_p/N_A}{dt} = k_{pw} C_w [IM^\bullet_{j_{crit}-1}] + \sum_{i=z}^{j_{crit}-1} k^i_{e,micelle} C_{micelle} [IM^\bullet_i] \tag{59}$$

where $C_{micelle}$ is the concentration of micelles in the aqueous phase. The value of $C_{micelle}$ can be found by considering the relationship between the total amount of surfactant added to the aqueous phase initially, the CMC and the amount adsorbed onto the particles, given by:

$$C_{micelle} = \text{maximum of} \left(\frac{[S] - \frac{4\pi r_s^2 N_p}{N_A a_s} - [CMC]}{n_{agg}} \right) \text{and } 0 \tag{60}$$

where n_{agg} is the aggregation number of the micelle (i.e. the number of surfactant molecules per micelle), and all other terms defined previously. Using well-defined values (for example, for Aerosol-MA80 (AMA-80) stabilized systems we have [CMC] = 10 mM [145], sodium dodecyl sulfate (SDS) parameters of $a_s = 0.43$ nm^2 [146], $r_{micelle} = 2.3$ nm and $n_{agg} = 162$ [147] also used in this case), N_p as a function of surfactant concentration can be predicted (the calculation is quite insensitive to the values of $r_{micelle}$ and n_{agg}). Comparison with experiment (unpublished data of P. Hidi, The University of Sydney) is given in Fig. 20. The model semi-quantitatively reproduces the experimentally determined particle numbers, and most importantly it demonstrates the expected sharp increase at the CMC (it should be noted, however, that experimentally the sharp increase is seen *around* the CMC; the reason that the sharp change predicted by the model is in fact a gentler one in experiment has been discussed above). The simple Smith–Ewart exponent of $[S]^{0.6}$ is also well reproduced by this model and by experiment *over a limited region*, but as has been shown [114] previously, any model that relies on the exhaustion of surfactant as the end of particle formation will demonstrate a similar exponent. As discussed elsewhere [2], it is well known that the value of the CMC changes somewhat in the presence of monomer and with ionic strength, but these effects merely make slight quantitative but not qualitative changes to the predicted behaviour (note the axis is logarithmic in [surfactant]).

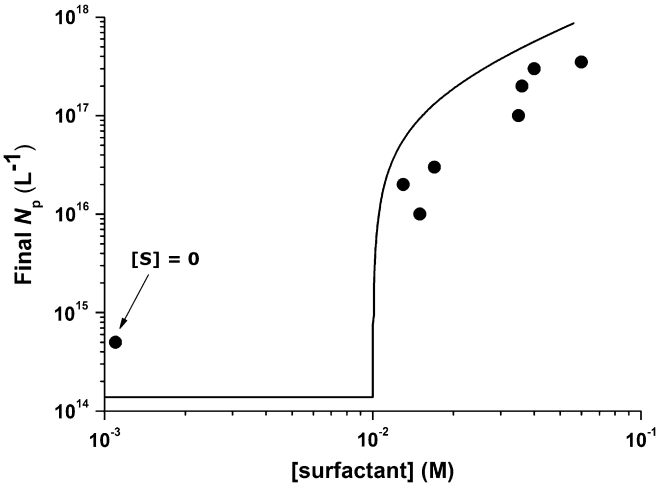

Fig. 20. Final particle number for *ab initio* emulsion polymerization of styrene as a function of [AMA-80] using the micellar nucleation model (323 K) with experimental comparison (black circles).

7.5. Particle formation in electrosterically stabilized systems

The particle formation mechanism for *ab initio* electrosterically stabilized systems is complicated by the presence of (at least) two monomers in the system – the hydrophobic monomer that comprises the majority of the particle and the hydrophilic monomer (typically an acid monomer such as acrylic acid (AA) or itaconic acid, or the neutral ethylene oxide) that will act as an anchored stabilizer on the surface of the particle. Ethylene oxide is always present as preformed surfactant (e.g. poly(ethylene oxide) nonylphenyl ether) while the AA or other vinylic monomers are added as co-monomer. Both monomers are likely to exhibit vastly different kinetics (for example, the propagation rate coefficient k_p of AA in water is up to 100 times larger than that of styrene [33]) and as a result the final N_p in such a co-monomer system will be dependent on monomer ratios, feed rates and many other significant factors. Both the polydispersity and the surface activity of the chains forming in the aqueous phase are hard to both predict and measure. Characterization of the hairy layer is difficult, with techniques such as small-angle neutron scattering (SANS) providing at best ambiguous results regarding the size of the hydrophilic block as a function of hydrophilic monomer concentration [35].

The advent of controlled-radical polymerization techniques applicable in emulsion systems have revealed much about the particle formation mechanism in electrosterically stabilized systems. The ability to perform controlled polymerization of hydrophilic monomers in water through the use for RAFT-based [37] and nitroxide-based [148–150] techniques has allowed for the first time the possibility of determining the dependence on the length of the hydrophilic block (as well as the length of the initial hydrophobic segment if considering *ab initio* reactions using diblock copolymers). This has provided considerable insight into the timescale of particle formation and the function of block length, especially using techniques such as on-line reaction calorimetry [128].

Under conditions where the monomer is fed into the reaction vessel in such systems as described above, there is a critical point where the diblock copolymers become surface active, and begin to self-assemble. This marks the beginning of the particle formation process; however [151], diblocks can migrate between the aggregated structures while they retain some degree of water solubility. As chains continue to grow in length, their ability to migrate will eventually cease – marking the end of particle formation. For example, with diblocks initially comprising 10 acrylic acid (AA) and 10 styrene units, the addition of 5 further styrene units renders the polymeric chain effectively unable to migrate [152]. The stages in particle formation in such systems are thus as follows:

- Step 1: aqueous-phase growth of water-soluble species, which become progressively more surface active;
- Step 2: self-assembly of these into micelles (or similar species), with migration of the species between micelles at the same time as these species continue to grow;
- Step 3: cessation of particle formation as either all species contain sufficiently hydrophobic components as to become immobile and/or sufficient particles of sufficient size to capture any migrating species before they can form new micelles.

This mechanism has been proposed as well as supported by the work of Barrett [153] in the field of dispersion polymerization in organic media, as well as numerous groups [154–157] who have investigated the use of di- and multi-block copolymers as stabilizers in emulsion polymerization, synthesized through a variety of different techniques. Recently, a simple model [127] was put forward to model the final particle number N_p as a function of initiator concentration and initial degree of polymerization of the hydrophobic component of the diblock copolymer, that is for systems starting in Step 2 of the above mechanism. The treatment is in the same vein as Smith–Ewart model, determining a critical point where all 'surfactant' has been captured by pre-existing particles. It assumes that aqueous-phase propagation and termination occur as outlined by Maxwell–Morrison mechanism [62] takes place, and that z-mers enter micelle-like species constantly over time, forming a particle (see Fig. 21). There exists a critical time t, however, where the degree of polymerization of the hydrophobic block reaches a critical length X_{crit} where migration is no longer possible – the evolution equation of the number-average degree of polymerization $\overline{X}_n$ is given by:

$$\frac{d\overline{X}_n}{dt} = \frac{k_p C_p \overline{n}}{n_{chains}} \tag{61}$$

where n_{chains} is the number of chains per particle (the ratio of the area of a particle A_s and the area per headgroup of a chain a_{chain}), with all other terms defined previously. Note that n_{chains} in Eq. (61) is not the aggregation number, but is the final number of chains per particle. Relating n_{chains} to the swollen area

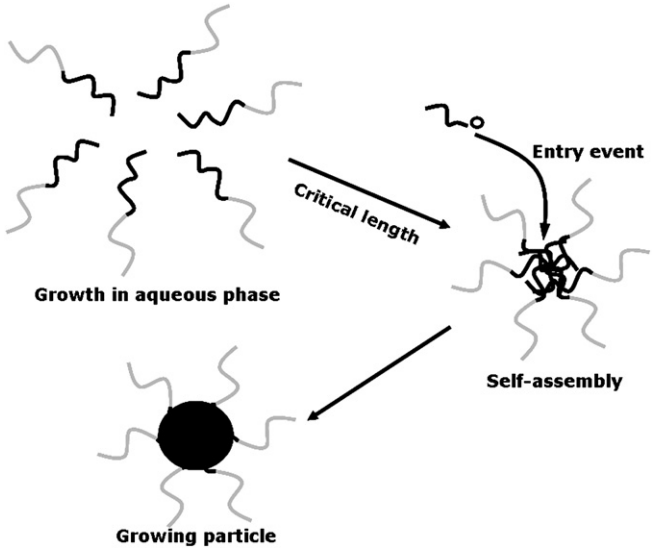

Fig. 21. Proposed mechanism of particle formation in RAFT-controlled self-assembly based *ab initio* systems.

(and hence volume) of a particle while assuming a time-independent $\bar{n}$ allows the critical time t to be determined when the critical length X_{crit} is attained, and as a result N_p can be estimated. Results demonstrated that agreement with experimentally attained particle number values for different length hydrophilic and hydrophobic blocks was acceptable [127], with the model showing a strong dependence on X_{crit}, $\overline{X}_n(t=0)$ and a_{chain}. The aggregation number of the original diblock copolymer has been shown to obey an empirical relation related to the length of the hydrophilic and hydrophobic blocks; the nature of the diblocks themselves dictates the relation between the number of micellar structures and the final particle number, which is discussed below.

While this model provides a starting point to rationalize the significant contributors to the particle formation mechanism in such systems, the hydrophilicity of the starting diblock copolymer adds a further layer of complication. Rager et al. [158] carried out emulsion polymerization experiments using AA–MMA diblock copolymers of varying composition as stabilizers in emulsion polymerization experiments, with the AA:MMA ratio varying from 0.33 to 3.5. For diblocks with a 1:1 AA:MMA ratio or lower, the exponent α that dictates the power dependence of the stabilizer concentration [S] was shown to be 1, suggesting frozen micellar-like structures that all lead to the formation of a particle. Similarly, diblocks with a higher hydrophilic content were seen to behave like typical low molecular weight surfactants, displaying the 'typical' Smith–Ewart power law dependence of 0.6. In analogous experiments performed by Burguière et al. [159] using AA–styrene diblocks, α was seen to be 1 for 'hydrophobic' diblocks with an AA content of less than 75%. The exchange dynamics of such structures above their CMC (which are typically very low) was thus shown to be crucial on the timescale of particle nucleation in determining the power law dependence on the stabilizer concentration. That is, in these 'frozen micelle' cases, the system starts directly in Step 3 in the mechanism given above.

7.6. Secondary nucleation in electrosterically stabilized systems

One of the more puzzling features of electrosterically stabilized emulsion systems is the extensive amount of secondary nucleation seen under certain reaction conditions, where according to both the homogeneous and the micellar nucleation mechanisms the amount of new particles formed should be negligible. In the poly(acrylic acid) stabilized styrene emulsion systems used by Vorwerg [58], secondary nucleation only occurred at neutral and high pH conditions; the amount of new particles, however, was over seven orders of magnitude higher than that predicted via homogeneous nucleation [2,160]. Similarly significant excess of new particles have been seen in poly(ethylene oxide) stabilized emulsion systems (unpublished data obtained by M Hammond, RG Gilbert and DH Napper in the University of Sydney), indicating a significant departure from the expected mechanisms that govern this process in such systems. One would anticipate that with a 10^7 increase in the number of new particles formed relative to the predictions of the well established particle formation models, a new, yet-to-be-discovered mechanism is taking place.

It has recently been postulated [65] that fragmentation of the stabilizing chain (through β-scission for example) may provide a significant increase in the number of 'nucleation sites' that can lead to new particles relative to the homogeneous nucleation mechanism (as polymerically/electrosterically stabilized systems are performed in the absence of any added surfactant). The role of mid-chain radicals in (electro)-sterically stabilized systems was discussed above. A mid-chain radical can potentially fragment (an event often blamed for the difficulty in obtaining reliable PLP data in acrylate systems [161] and that has been observed in pulse-radiolysis experiments on poly(AA) [162]) and thus a poly(AA) chain with either a radical or an unsaturated end group can move into the aqueous phase. Further interaction with aqueous-phase radical species (transfer, termination, etc.) may lead to the generation of a precursor particle; work is currently underway to determine the significance of this β-scission event in the particle formation process. This naturally is far from definitive (issues remain regarding the rate of β-scission at the reaction temperatures in question and the actual likelihood that such a mechanism would lead to new particle formation). While this postulate is consistent with all available data, it has not been definitively proved or refuted, and obtaining new experimental data is crucial in attempting to explain such unusual results in this area of emulsion polymerization.

8. Conclusions

In this review, a comprehensive analysis of the kinetics of emulsion polymerization has been presented, as well as an account of the experiments used to help determine critical rate coefficients and elucidate mechanisms. The fundamental interfacial processes of radical entry and exit are well understood for both electrostatically and electrosterically stabilized latexes; similarly the mechanisms that govern the formation of emulsion particles both above and below the CMC (in the case of traditional surfactants) as well as in the presence of diblock copolymer stabilizers are well understood. These studies complement the work done to fundamentally understand the key reactions that govern any polymerization reaction – initiation, propagation, transfer and termination – and in doing so create an essentially complete picture of emulsion polymerization kinetics. It is hoped that through this fundamental understanding, novel structures and systems can be created with optimized properties specific for a relevant application.

Acknowledgements

The financial support of a Discovery Grant from the Australian Research Council and an Australian Postgraduate Award (APA) are gratefully acknowledged, as is a grant provided by the Australian Institute of Nuclear Science and Engineering (AINSE) and a Surface Coatings Association of Australia scholarship.

References

[1] Urban D, Takamura K. Polymer dispersions and their industrial applications. Weinheim: Wiley-VCH; 2002.
[2] Gilbert RG. Emulsion polymerisation: a mechanistic approach. San Diego: Academic Press; 1995.
[3] Adams ME, Trau M, Gilbert RG, Napper DH, Sangster DF. Aust J Chem 1988;41:1799.
[4] Olaj OF, Bitai I. Angew Makromol Chem 1987;155:177.
[5] Gilbert RG. Pure Appl Chem 1992;64:1563.
[6] Buback M, Gilbert RG, Hutchinson RA, Klumperman B, Kuchta F-D, Manders BG, et al. Macromol Chem Phys 1995;196:3267.
[7] van Herk AM. Macromol Theory Simul 1998;7:557.
[8] Harkins WD. J Am Chem Soc 1947;69:1428.
[9] Morton M, Kaizerman S, Altier MW. J Colloid Sci 1954;9:300.
[10] Hawkett BS, Napper DH, Gilbert RG. J Chem Soc Faraday Trans 1 1981;77:2395.
[11] Norrish RGW, Smith RR. Nature 1942;150:336.
[12] Trommsdorff E, Kohle E, Lagally P. Makromol Chem 1948;1:169.
[13] Coen EM, Lyons RA, Gilbert RG. Macromolecules 1996;29:5128.
[14] Smith WV, Ewart RH. J Chem Phys 1948;16:592.
[15] van Berkel KY, Russell GT, Gilbert RG. Macromolecules 2005;38:3214.
[16] Ugelstad J, Hansen FK. Rubber Chem Technol 1976;49:536.
[17] Ballard MJ, Gilbert RG, Napper DH. J Polym Sci Polym Lett Ed 1981;19:533.
[18] Buback M, Egorov M, Gilbert RG, Kaminsky V, Olaj OF, Russell GT, et al. Macromol Chem Phys 2002;203:2570.
[19] Clay PA, Gilbert RG. Macromolecules 1995;28:552.
[20] Prescott SW, Ballard MJ, Gilbert RG. J Polym Sci Part A Polym Chem 2005;43:1076.
[21] Casey BS, Morrison BR, Maxwell IA, Gilbert RG, Napper DH. J Polym Sci Part A Polym Chem 1994;32:605.
[22] McAuliffe C. J Phys Chem 1966;70:1267.
[23] Nomura M, Harada M. J Appl Polym Sci 1981;26:17.
[24] Lane WH. Ind Eng Chem 1946;18:295.
[25] Heuts JPA, Radom L, Gilbert RG. Macromolecules 1995;28:8771.
[26] Casey BS, Morrison BR, Gilbert RG. Prog Polym Sci 1993;18:1041.
[27] Morrison BR, Casey BS, Lacík I, Leslie GL, Sangster DF, Gilbert RG, et al. J Polym Sci Part A Polym Chem 1994;32:631.
[28] Maeder S, Gilbert RG. Macromolecules 1998;31:4410.
[29] Prescott SW. Macromolecules 2003;36:9608.
[30] Ballard MJ, Napper DH, Gilbert RG. J Polym Sci Polym Chem Ed 1984;22:3225.
[31] Russell GT. Macromol Theory Simul 1994;3:439.
[32] Smith GB, Russell GT, Heuts JPA. Macromol Theory Simul 2003;12:299.
[33] Lacik I, Beuermann S, Buback M. Macromolecules 2003;36:9355.
[34] Lacik I, Beuermann S, Buback M. Macromol Chem Phys 2004;205:1080.
[35] De Bruyn H, Gilbert RG, White JW, Schulz JC. Polymer 2003;44:4411.
[36] Save M, Guillaneuf Y, Gilbert RG. Aust J Chem 2006;59:693.
[37] Ferguson CJ, Hughes RJ, Nguyen D, Pham BTT, Hawkett BS, Gilbert RG, et al. Macromolecules 2005;38:2191.
[38] Ferguson CJ, Hughes RJ, Pham BTT, Hawkett BS, Gilbert RG, Serelis AK, et al. Macromolecules 2002;35:9243.
[39] Chiefari J, Chong YK, Ercole F, Krstina J, Le TPT, Mayadunne RTA, et al. Macromolecules 1998;31:5559.
[40] Prescott SW, Ballard MJ, Rizzardo E, Gilbert RG. Macromolecules 2002;35:5417.
[41] Elizalde O, Azpeitia M, Reis MM, Asua JM, Leiza JR. Ind Eng Chem Res 2005;44:7200.
[42] Verdurmen EM, German AL, Sudol ED, Gilbert RG. Macromol Chem Phys 1994;195:635.
[43] De La Rosa LV, Sudol ED, El-Aasser MS, Klein A. J Polym Sci Part A Polym Chem 1996;34:461.
[44] De La Rosa LV, Sudol ED, El-Aasser MS, Klein A. J Polym Sci Part A Polym Chem 1999;37:4073.
[45] De La Rosa LV, Sudol ED, El-Aasser MS, Klein A. J Polym Sci Part A Polym Chem 1999;37:4066.
[46] De La Rosa LV, Sudol ED, El-Aasser MS, Klein A. J Polym Sci Part A Polym Chem 1999;37:4054.
[47] Ozdeger E, Sudol ED, El-Aasser MS, Klein A. J Polym Sci Part A Polym Chem 1997;35:3837.
[48] Ozdeger E, Sudol ED, El-Aasser MS, Klein A. J Polym Sci Part A Polym Chem 1997;35:3813.
[49] Ozdeger E, Sudol ED, El-Aasser MS, Klein A. J Polym Sci Part A Polym Chem 1997;35:3827.
[50] Blythe PJ, Klein A, Phillips JA, Sudol ED, El-Aasser MS. J Polym Sci Part A Polym Chem 1999;37:4449.
[51] Lamb DJ, Fellows CM, Morrison BR, Gilbert RG. Polymer 2005;46:285.
[52] McAskill NA, Sangster DF. Aust J Chem 1984;37:2137.
[53] Lansdowne SW, Gilbert RG, Napper DH, Sangster DF. J Chem Soc Faraday Trans 1 1980;76:1344.
[54] Christie DI, Gilbert RG, Congalidis JP, Richards JR, McMinn JH. Macromolecules 2001;34:5158.
[55] van Berkel KY, Russell GT, Gilbert RG. Macromolecules 2003;36:3921.
[56] Tobolsky AV, Offenbach J. J Polym Sci 1955;16:311.
[57] Willemse RXE, Staal BBP, van Herk AM, Pierik SCJ, Klumperman B. Macromolecules 2003;36:9797.
[58] Vorwerg L, Gilbert RG. Macromolecules 2000;33:6693.
[59] Thickett SC, Gilbert RG. Macromolecules 2006;39:2081.
[60] Asua JM. Macromolecules 2003;36:6245.
[61] Thickett SC, Gilbert RG. Macromolecules 2006;39:6495.
[62] Maxwell IA, Morrison BR, Napper DH, Gilbert RG. Macromolecules 1991;24:1629.
[63] Guillet JE, Burke NAD. Canada Patent 98-2249955 2249955; 2000.
[64] Loiseau J, Doërr N, Suau JM, Egraz JB, Llauro MF, Ladavière C. Macromolecules 2003;36:3066.
[65] Thickett SC, Gaborieau M, Gilbert RG. Macromolecules 2007;40:4710.
[66] Bromberg LE, Barr DP. Macromolecules 1999;32:3647.
[67] Hawkett BS, Napper DH, Gilbert RG. J Chem Soc Faraday Trans 1 1980;76:1323.
[68] Halnan LF, Napper DH, Gilbert RG. J Chem Soc Faraday Trans 1 1984;80:2851.
[69] Fitch RM, Shih L. Prog Colloid Polym Sci 1975;56:1.
[70] Yeliseeva VI. In: Piirma I, editor. Emulsion polymerization. New York: Academic; 1982. p. 247.
[71] Penboss IA, Gilbert RG, Napper DH. J Chem Soc Faraday Trans 1 1986;82:2247.
[72] Maxwell IA, Morrison BR, Napper DH, Gilbert RG. Makromol Chem 1992;193:303.
[73] De Bruyn H, Miller CM, Bassett DR, Gilbert RG. Macromolecules 2002;35:8371.
[74] Zammit MD, Davis TP, Haddleton DM, Suddaby KG. Macromolecules 1997;30:1915.
[75] Davies JT, Rideal EK. Interfacial phenomena. New York: Academic; 1961.
[76] Marestin C, Guyot A, Claverie J. Macromolecules 1998;31:1686.
[77] Plyasunov AV, Shock EL. J Supercrit Fluids 2001;20:91.
[78] Morrison BR, Maxwell IA, Gilbert RG, Napper DH. In: Daniels ES, Sudol ED, El-Aasser M, editors. Polymer latexes – preparation, characterization and applications. ACS symposium series. Washington, DC: American Chemical Society; 1992. p. 28.
[79] Hernandez HF, Tauer K. Ind Eng Chem Res 2007;46:4480.
[80] Asua JM, De la Cal JC. J Appl Polym Sci 1991;42:1869.
[81] Kim JU, Lee HH. Macromolecules 1994;27:3337.
[82] Kshirsagar RS, Poehlein GW. J Appl Polym Sci 1994;54:909.
[83] Dong Y, Sundberg DC. Macromolecules 2002;35:8185.
[84] Dong Y. J Colloid Interface Sci 2005;288:390.
[85] Tauer K, Nozari S, Ali AMI. Macromolecules 2005;38:8611.
[86] Goicoechea M, Barandiaran MJ, Asua JM. Macromolecules 2006;39:5165.
[87] Plessis C, Arzamendi G, Leiza JR, Schoonbrood HAS, Charmot D, Asua JM. Macromolecules 2000;33:4.

[88] Ahmad NM, Heatley F, Lovell PA. Macromolecules 1998;31:2822.
[89] Beuermann S, Buback M, Schmaltz C. Macromolecules 1998;31:8069.
[90] Thickett SC, Gilbert RG. Macromolecules 2005;38:9894.
[91] Barner-Kowollik C, Buback M, Egorov M, Fukuda T, Goto A, Olaj OF, et al. Prog Polym Sci 2005;30:605.
[92] Benson SW, North AM. J Am Chem Soc 1962;84:935.
[93] Gilbert RG, Smith SC. Theory of unimolecular and recombination reactions. Melbourne: Blackwell Scientific; 1990.
[94] Russell GT. Aust J Chem 2002;55:399.
[95] Ballard MJ, Napper DH, Gilbert RG, Sangster DF. J Polym Sci Polym Chem Ed 1986;24:1027.
[96] Tirrell M. Rubber Chem Technol 1984;57:523.
[97] Lovestead TM, Theis A, Davis TP, Stenzel MH, Barner-Kowollik C. Macromolecules 2006;39:4975.
[98] Theis A, Feldermann A, Charton N, Stenzel MH, Davis TP, Barner-Kowollik C. Macromolecules 2005;38:2595.
[99] Johnston-Hall G, Stenzel MH, Davis TP, Barner-Kowollik C, Monteiro MJ. Macromolecules 2007;40:2730.
[100] Russell GT. Macromol Theory Simul 1995;4:497.
[101] Russell GT. Macromol Theory Simul 1995;4:519.
[102] Russell GT. Macromol Theory Simul 1995;4:549.
[103] Russell GT, Gilbert RG, Napper DH. Macromolecules 1992;25:2459.
[104] Russell GT, Gilbert RG, Napper DH. Macromolecules 1993;26:3538.
[105] Griffiths MC, Strauch J, Monteiro MJ, Gilbert RG. Macromolecules 1998;31:7835.
[106] Strauch J, McDonald J, Chapman BE, Kuchel PW, Hawkett BS, Roberts GE, et al. J Polym Sci Part A Polym Chem 2003;41:2491.
[107] Piton MC, Gilbert RG, Chapman BE, Kuchel PW. Macromolecules 1993;26:4472.
[108] Russell GT, Napper DH, Gilbert RG. Macromolecules 1988;21:2133.
[109] Scheren PAGM, Russell GT, Sangster DF, Gilbert RG, German AL. Macromolecules 1995;28:3637.
[110] Smith GB, Heuts JPA, Russell GT. Macromol Symp 2005;226:133.
[111] Clay PA, Christie DI, Gilbert RG. In: Matyjaszewski K, editor. Advances in free-radical polymerization. Washington, DC: ACS; 1998. p. 104.
[112] Smith GB, Russell GT. Macromol Symp 2007;248:1.
[113] Adams ME, Russell GT, Casey BS, Gilbert RG, Napper DH, Sangster DF. Macromolecules 1990;23:4624.
[114] Roe CP. Ind Eng Chem 1968;60:20.
[115] Fitch RM. Br Polym J 1973;5:467.
[116] Gardon JL. J Polym Sci Polym Chem Ed 1968;6:643.
[117] Gardon JL. J Polym Sci Polym Chem Ed 1968;6:687.
[118] Landfester K. Macromol Symp 2000;150:171.
[119] Prescott SW, Ballard MJ, Rizzardo E, Gilbert RG. Aust J Chem 2002; 55:415.
[120] Kukulj D, Gilbert RG. In: Asua JM, editor. Polymeric dispersions: principles and applications. Dordrecht: Kluwer Academic; 1997. p. 97.
[121] Hergeth WD, Lebek W, Kakuschke R, Schmutzler K. Makromol Chem 1991;192:2265.
[122] Hergeth WD, Lebek W, Stettin E, Witkowski K, Schmutzler K. Makromol Chem 1992;193:1607.
[123] Feeney PJ, Napper DH, Gilbert RG. Macromolecules 1984;17:2520.
[124] Feeney PJ, Napper DH, Gilbert RG. Macromolecules 1987;20:2922.
[125] Fitch RM, Watson RC. J Colloid Interface Sci 1979;68:14.
[126] Morrison BR, Maxwell IA, Gilbert RG, Napper DH. ACS Symp Ser 1992;492:28.
[127] Gilbert RG. Macromolecules 2006;39:4256.
[128] Sprong E, Leswin JS, Lamb DJ, Ferguson CJ, Hawkett BS, Pham BT, et al. Macromol Symp 2006;231:84.
[129] Priest WJ. J Phys Chem 1952;56:1077.
[130] Fitch RM, Tsai CH. In: Fitch RM, editor. Polymer colloids. New York: Plenum; 1971. p. 73.
[131] Goodall AR, Wilkinson WC, Hearn J. J Polym Sci Polym Chem Ed 1977;15:2193.
[132] Goodwin JW, Hearn J, Ho CC, Ottewill RH. Colloid Polym Sci 1974; 252:464.
[133] Barouch E, Matijevic E. J Chem Soc Faraday Trans 1 1985;81:1797.
[134] Barouch E, Matijevic E, Wright TH. J Chem Soc Faraday Trans 1 1985; 81:1819.
[135] Morrison BR, Gilbert RG. Macromol Symp 1995;92:13.
[136] Coen EM, Gilbert RG, Morrison BR, Peach S, Leube H. Polymer 1998; 39:7099.
[137] Ferguson CJ, Russell GT, Gilbert RG. Polymer 2002;43:4545.
[138] Prescott S, Gilbert RG. Macromol Theory Simul 2002;11:163.
[139] Chern CS, Lin CH. Polymer 1998;40:139.
[140] Sütterlin N. In: Fitch RM, editor. Polymer colloids II. New York: Plenum; 1980. p. 583.
[141] Coen EM, Morrison BR, Peach S, Gilbert RG. Polymer 2004;45:3595.
[142] Song Z, Poehlein GW. J Colloid Interface Sci 1989;128:486.
[143] Song Z, Poehlein GW. J Colloid Interface Sci 1989;128:501.
[144] Song Z, Poehlein GW. J Polym Sci Part A Polym Chem 1990;28:2359.
[145] Jobe DJ, Reinsborough VC. Can J Chem 1984;62:280.
[146] Ahmed SM, El-Aasser MS, Micale FJ, Poehlein GW, Vanderhoff JW. In: Fitch RM, editor. Polymer colloids II. New York: Plenum; 1980. p. 265.
[147] Giannetti E. AIChE J 1993;39:1210.
[148] Delaittre G, Nicolas J, Lefay C, Save M, Charleux B. Chem Commun 2005:614.
[149] Nicolas J, Charleux B, Guerret O, Magnet S. Angew Chem Int Ed 2004; 43:6186.
[150] Nicolas J, Charleux B, Guerret O, Magnet S. Macromolecules 2004;37: 4453.
[151] Israelachvili JN. Intermolecular and surface forces. 2nd ed. London: Academic; 1992.
[152] Pham BTT, Nguyen D, Ferguson CJ, Hawkett BS, Serelis AK, Such CH. Macromolecules 2003;36:8907.
[153] Barrett KEJ. Br Polym J 1973;5:259.
[154] Garnier S, Laschewsky A. Macromolecules 2005;38:7580.
[155] Garnier S, Laschewsky A. Langmuir 2006;22:4044.
[156] Save M, Manguian M, Chassenieux C, Charleux B. Macromolecules 2005;38:280.
[157] Tauer K, Zimmermann A, Schlaad H. Macromol Chem Phys 2002; 203:319.
[158] Rager T, Meyer WH, Wegner G, Mathauer K, Machtle W, Schrof W, et al. Macromol Chem Phys 1999;200:1681.
[159] Burguière C, Pascual S, Bui C, Vairon J-P, Charleux B, Davis KA, et al. Macromolecules 2001;34:4439.
[160] Hansen FK, Ugelstad J. In: Piirma I, editor. Emulsion polymerization. New York: Academic; 1982.
[161] van Herk AM. Macromol Rapid Commun 2001;22:687.
[162] von Sonntag C, Bothe E, Ulanski P, Deeble DJ. Radiat Phys Chem 1995;46:527.

Glossary of symbols and abbreviations

α: exponent relating the particle number to surfactant concentration;
A: collection of constants from seeded Interval II emulsion polymerization (s^{-1});
a: intercept of fit to linear region of conversion–time curve;
a: root-mean-square end-to-end distance per square root of the number of monomer units in a polymer chain (nm);
AA: acrylic acid;
A_p: critical area of a particle where all surfactants are adsorbed onto the particle surface;
a_s: area occupied by a single surfactant molecule on the particle surface (nm^2);
A_s: area of a single latex particle;
b: slope of fit to linear region of conversion–time curve (s^{-1});
$\langle c \rangle$: chain-length average first-order termination rate coefficient (s^{-1});
c: pseudo-first-order rate coefficient for bimolecular termination (s^{-1});
c^{**}: concentration of polymer at which chains are entangled;
CMC: critical micelle concentration (M);
$C_{micelle}$: concentration of micelles (M);
C_p: monomer concentration within the particle phase (M);

C_p^{sat}: saturation concentration of monomer in the particle phase (M);
C_w: monomer concentration within the aqueous phase (M);
C_w^{sat}: saturation concentration of monomer in the aqueous phase (M);
D_h: diffusion coefficient within the 'hairy layer' of an electrosterically stabilized latex ($m^2\,s^{-1}$);
D_i^{com}: centre-of-mass diffusion coefficient of an i-meric radical ($m^2\,s^{-1}$);
D_{mon}: diffusion coefficient of a monomeric unit ($m^2\,s^{-1}$);
d_p: density of the polymer ($g\,mL^{-1}$);
D^{rd}: reaction-diffusion coefficient by propagational growth ($m^2\,s^{-1}$);
D_w: diffusion coefficient of a radical in the aqueous phase ($m^2\,s^{-1}$);
f: decomposition efficiency of initiator;
Γ: interfacial tension between latex particles;
$[I]$: initiator concentration (M);
IM_i^*: aqueous-phase oligomer containing i monomer units;
j_{crit}: critical length of an oligomer where it is no longer soluble in the aqueous phase;
k: pseudo-first-order rate coefficient for radical exit (desorption) of a single free radical from a latex particle (s^{-1});
K: rate of volume of growth per particle;
$\langle k_t \rangle$: chain-length average second-order termination rate coefficient ($M^{-1}\,s^{-1}$);
k_{cr}: Limit 2a exit rate coefficient (s^{-1});
k_{ct}: Limit 1 exit rate coefficient (s^{-1});
k_d: rate coefficient for decomposition of initiator (s^{-1});
k_{dM}: rate coefficient for desorption of a monomeric radical from a particle (s^{-1});
k_e: second-order rate coefficient for entry ($M^{-1}\,s^{-1}$);
k_p: propagation rate coefficient ($M^{-1}\,s^{-1}$);
k_p^1: rate coefficient for propagation of a monomeric radical ($M^{-1}\,s^{-1}$);
k_{pi}: rate coefficient for addition of the monomer to initiator-derived fragment ($M^{-1}\,s^{-1}$);
k_{pw}: rate coefficient for propagation of monomer in the aqueous phase ($M^{-1}\,s^{-1}$);
k_{re}: second-order rate coefficient for re-entry of a monomeric radical ($M^{-1}\,s^{-1}$);
k_t^{ij}: termination rate coefficient for reaction between radicals of length i and j ($M^{-1}\,s^{-1}$);
k_{tr}: rate coefficient for transfer to monomer ($M^{-1}\,s^{-1}$);
k_{tw}: rate coefficient for termination in the aqueous phase ($M^{-1}\,s^{-1}$);
M: monomer unit;
M_0: molecular weight of the monomer;
MCR: mid-chain radical;
MMA: methyl methacrylate;
m_p^0: mass of the polymer per unit volume ($g\,mL^{-1}$);
$\bar{n}$: average number of radicals per particle;
$\bar{n}_0$: average number of radicals per particle at time $t = 0$;
$\bar{n}_t$: final steady-state value of average number of radicals per particle;
$\bar{n}_i$: initial steady-state value of average number of radicals per particle;
$\bar{n}_{ss}$: steady-state average number of radicals per particle;
N_0: number of particles containing no growing radicals;
N_1^m: number of particles containing one monomeric radical;
N_1^p: number of particles containing one polymeric radical;
N_A: Avogadro's constant (mol^{-1});
n_{agg}: aggregation number of a surfactant;
n_M^0: initial number of moles of monomer per unit volume (M);
N_n: number of particles containing n growing radicals;
N_p: concentration of polymer particles per unit volume of the aqueous phase (L^{-1});
p: probability of reaction upon encounter of radicals;
ρ: pseudo-first-order rate coefficient for entry from the aqueous phase (s^{-1});
ρ_{init}: component of first-order entry rate coefficient from chemical initiator (s^{-1});
ρ_{re}: rate coefficient for re-entry of an exited radical into a particle (s^{-1});
ρ_{spont}: component of first-order entry rate coefficient from spontaneous polymerization (s^{-1});
R_i: concentration of radicals of degree of polymerization i (M);
$r_{micelle}$: radius of a micelle (nm);
r_s: monomer-swollen particle radius (nm);
r_u: number-average unswollen particle radius (nm);
σ: Lennard-Jones diameter of a monomer unit (nm);
$[S]$: surfactant concentration (M);
V_s: swollen volume of a latex particle (nm^3);
w_p: weight fraction of the polymer;
χ: Flory–Huggins interaction parameter;
x: fractional conversion of monomer into polymer;
X_{crit}: critical length of hydrophobic block where migration is no longer possible;
$\overline{X}_n$: average degree of polymerization of hydrophobic block;
z: degree of polymerization to attain surface activity.

Stuart Thickett received his science degree, majoring in chemistry and pure mathematics, from the University of Sydney, Australia in 2002. He then attained his honours degree at the Key Centre for Polymer Colloids in 2003 under the supervision of Professor Bob Gilbert, focussing on *ab initio* quantum chemical modelling of the propagation step of acrylic acid – work for which he received the University Medal. He is now currently completing his Ph.D. at the same institution, working in the area of emulsion polymerization kinetics and the role of polymeric and electrosteric stabilization.

Professor Robert G (Bob) Gilbert is a Research Professor in the Centre for Nutrition and Food Science, University of Queensland. He received his undergraduate training at Sydney University, graduating in 1966, and his Ph.D. from the Australian National University, graduating in 1970. He carried out postdoctoral work at MIT in the US from 1970 to 1972, and then returned to the University of Sydney, where prior to his move to UQ, he was Director of the Key Centre for Polymer Colloids. He is a Fellow of the Australian Academy of Science, is author of 340 papers, 4 patents, and 2 books (on unimolecular reactions and on emulsion polymerization). He has worked on understanding the fundamental mechanisms in emulsion polymerization. Recently, he has extended this knowledge of *synthetic* polymers to the understanding and characterizing of branched polymers, particularly starch. This has led to unique combined experiment and theoretical methods for characterizing the complex molecular architecture of this biopolymer, and his move to UQ enables this research to gain from synergies with the Centre for Nutrition and Food Sciences.